

Electronic polarons and bipolarons in Fe-based superconductors: a pairing mechanism

Mona Berciu, Ilya Elfimov and George A. Sawatzky

Department of Physics and Astronomy, University of British Columbia, Vancouver B.C. V6T 1Z1, Canada

Superconductivity is a fascinating example of how “more is different” [1]. It is due to electrons binding into bosonic Cooper pairs, which exhibit coherent behavior across a macroscopic sample. Finding the mechanism responsible for this binding is one of the more difficult tasks of condensed matter physics. For conventional superconductors the solution was given by the BCS theory [2] as being due to exchange of phonons. For the cuprate high- T_c superconductors a widely-accepted explanation is still missing despite intense effort. The recently discovered Fe-based high- T_c superconductors pose now a new challenge [3, 4, 5, 6, 7]. We present here a quantum mechanical theory for pnictides describing the influence of the large electronic polarizability of the heavy anions. We demonstrate that its inclusion results in electronic polarons as the low-energy quasi-particles and also unveils a pairing mechanism for these electronic polarons.

At first sight, one may expect the pairing mechanism of pnictides to be related to that of the cuprates, given the somewhat similar layered structures. However, there is an essential difference between the CuO_2 layer where the important physics takes place in a cuprate, and its counterpart, the FeAs layer of a pnictide: while the former is two-dimensional (2D), with all Cu and O atoms in the same layer, the latter is not. Instead, the layer hosting the Fe atoms (which are arranged on a simple square lattice) is sandwiched between two layers which share equally the As atoms, as sketched in Fig. 1(a). Each Fe has 4 nearest neighbor (nn) As atoms at a distance $R = 2.4\text{\AA}$, arranged in a somewhat distorted tetrahedron, two in the upper and two in the lower layer.

The different geometry has important consequences. In the cuprates, the states near the Fermi energy consist of strongly hybridized Cu $3d$ and O $2p$ orbitals. In contrast, hardly any hybridization appears between the Fe $3d$ and As $4p$ orbitals, with the former giving essentially all the contribution to the low-energy states of the pnictides [8]. This lack of hybridization is due not only to the lattice structure but also to the substantial spread in space of $4p$ orbitals, as compared to $2p$ orbitals.

As a result, one might assume that the simplest Hamiltonian describing the low-energy physics of pnictides is a Hubbard Hamiltonian for the Fe $3d$ electrons, namely:

$$\mathcal{H}_{\text{Fe}} = - \sum_{i,j,\sigma} \left(t_{ij} c_{i,\sigma}^\dagger c_{j,\sigma} + h.c. \right) + U_H \sum_i \hat{n}_{i\uparrow} \hat{n}_{i\downarrow} \quad (1)$$

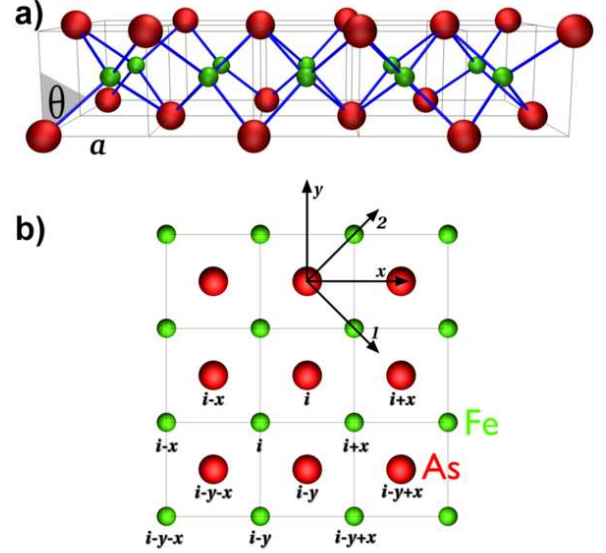


FIG. 1: (a) 3D sketch of the idealized FeAs layer. The lattice constant $a = 2.8\text{\AA}$ and angle θ (see text) are indicated; (b) Top view of the same Fe-As layer. Several sites are indexed. The Fe and As atoms are at different “depths”.

where $c_{i,\sigma}^\dagger$ creates an electron on the Fe site i with spin σ and $\hat{n}_{i\sigma} = c_{i\sigma}^\dagger c_{i\sigma}$. For simplicity, here we only count “doping” electrons, i.e. extra charges on top of the $3d^6$ configuration of the Fe in the undoped compound. Of course, a multiple-band Hamiltonian can also be used for the proper description of the various $3d$ orbitals, however the essential physics we want to discuss is already captured within this simpler starting point. The hopping integral is certainly finite for nn Fe sites, with $t_{i,i+x} = t$. We will also consider the effects of including 2^{nd} nn hopping, with $t_{i,i+x+y} = t'$ [the indexing of various sites is indicated in Fig. 1(b)]. The hopping to As sites is neglected, given the small hybridization.

Of course, Hamiltonian (1) is the most common starting point for cuprates (where it does include the O contribution, as $c_{i,\sigma}^\dagger$ are operators for Zhang-Rice singlets [9]). In contrast, using (1) or a similar starting point either in the strong-coupling [10, 11, 12, 13, 14, 15] or weak-coupling limit [16, 17, 18, 19] as the low-energy Hamiltonian for pnictides implies that the As anions play no role in their physics.

However, the As atoms are not irrelevant. As pointed out recently in Ref. 8, these are big, highly-polarizable ions which are strongly influenced by the extra charges

in their vicinity. One expects each such charge to be surrounded by polarized As ions, giving rise to *electronic polarons*. This results in a strong screening of the onsite Coulomb repulsion, suggesting that these materials are not in the large U limit of a Mott-Hubbard insulator. It also results in a strong nn attraction, which may be the key component in the pairing mechanism. The arguments of Ref. 8 are based on semi-classical estimates. Here we propose a quantum model which allows us to investigate this phenomenology away from the linear regime, and to also study dynamic properties of these polarons and bound bipolarons.

The polarization of the As^{3-} ions by the electric fields of the external charges is due to matrix elements coupling their filled $4p$ to (primarily) their empty $5s$ orbitals (more details are in the supplementary material). This is equivalent to a hole being virtually excited from the $5s$ into the $4p$ orbitals. We therefore describe each As by 4 operators: $s_{\sigma}^{\dagger}, p_{x,\sigma}^{\dagger}, p_{y,\sigma}^{\dagger}, p_{z,\sigma}^{\dagger}$, which create a hole of spin σ in the respective orbital. The ground-state of an As ion is $s_{\uparrow}^{\dagger}s_{\downarrow}^{\dagger}|0\rangle$ and the p -orbitals lie at an energy Ω above it, so that the unperturbed As ions are described by:

$$\mathcal{H}_{\text{As}} = \Omega \sum_{i,\lambda,\sigma} p_{i,\lambda,\sigma}^{\dagger} p_{i,\lambda,\sigma}, \quad (2)$$

where i is the location of the As ion [see Fig. 1(b)] $\lambda = x, y, z$ and σ is the spin of the hole. Hopping between As ions is very small, given the large nn distance between them of about 4\AA , and we ignore it. Indeed, LDA calculations find narrow $4p$ bands [8], justifying this atomistic description of the As ions.

We make two approximations regarding the interactions: (i) only As atoms nn to an Fe hosting a charge are polarized by its electric field, and (ii) we ignore dipole-dipole interactions between As clouds. (Estimates of the corresponding corrections are given in the supplementary material). Our interaction Hamiltonian is, then:

$$\begin{aligned} \mathcal{H}_{\text{int}} = & g \sum_{i,\sigma} \hat{n}_i \left[s_{i,\sigma}^{\dagger} (-\sin\theta p_{i,2,\sigma} + \cos\theta p_{i,3,\sigma}) \right. \\ & + s_{i-y,\sigma}^{\dagger} (-\sin\theta p_{i-y,1,\sigma} - \cos\theta p_{i-y,3,\sigma}) \\ & + s_{i-x-y,\sigma}^{\dagger} (\sin\theta p_{i-x-y,2,\sigma} + \cos\theta p_{i-x-y,3,\sigma}) \\ & \left. + s_{i-x,\sigma}^{\dagger} (\sin\theta p_{i-x,1,\sigma} - \cos\theta p_{i-x,3,\sigma}) + h.c. \right] \quad (3) \end{aligned}$$

where the sum is over all unit cells i in the lattice. This interaction describes the $5s \leftrightarrow 4p$ transitions resulting in the polarization of the As along the appropriate Fe-As direction (see Fig. 1) if doping charges, counted by $\hat{n}_i = \hat{n}_{i\uparrow} + \hat{n}_{i\downarrow}$, are on any Fe_i site.

Our model Hamiltonian $\mathcal{H} = \mathcal{H}_{\text{Fe}} + \mathcal{H}_{\text{As}} + \mathcal{H}_{\text{int}}$ is characterized by 5 energy scales. The hopping integral $t = 0.25\text{eV}$ and the $5s - 4p$ energy difference $\Omega = 6\text{eV}$ are estimated from LDA results (for details on determining all the parameters, see the supplementary material).

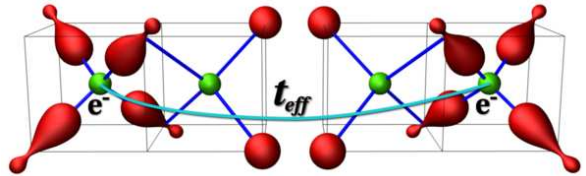


FIG. 2: Sketch of a single electronic polaron and its nn hopping. The electric field created by the extra electron residing on the Fe excites holes of nn As into the $4p$ orbital pointing towards the Fe (more distant As atoms stay in the $5s$ ground state). The hopping integral is renormalized by the overlap of the polarization clouds in the initial and final states.

We use either $t' = 0$ or $t' = -t/2$, the latter being the appropriate value for hopping between d_{xy}, d_{xz}, d_{yz} orbitals which contribute most near the Fermi level. The interaction energy $g = 2.5\text{eV}$ is extracted from the As^{3-} polarizability $\alpha_p = 10\text{\AA}^3$, and the Hubbard onsite repulsion U_H is left as a free parameter. We present results for a wide range of these parameters, proving that our results are only weakly sensitive to their precise values.

We begin with a study of the low-energy spectrum of the electronic polaron [sketched in Fig. 2] created when there is one doping electron in the system. We use first order perturbation theory in the hopping, which is the smallest energy (a quantitative justification and full details of the calculations are provided in the supplementary material). The polaron eigenenergies are:

$$E_P(\vec{k}) = 4(\Omega - \sqrt{\Omega^2 + 4g^2}) + \epsilon_{\text{eff}}(\vec{k}). \quad (4)$$

The first term is the interaction energy between the electron and the induced As dipole moments. For $g \ll \Omega$ it equals $-4[\alpha_p E^2/2] \approx -8.2\text{eV}$, E being the electric field at the As sites. This linear expression was used in Ref. 8. Since in fact $g/\Omega \approx 0.4$, non-linear effects become important and reduce it slightly to $\approx -7.1\text{eV}$. $\epsilon_{\text{eff}}(\vec{k}) = -2t_{\text{eff}} [\cos(k_x a) + \cos(k_y a)] - 4t'_{\text{eff}} \cos(k_x a) \cos(k_y a)$ is a dispersion identical to that of a free particle, but with renormalized hopping integrals due to the overlap of the As clouds as the polaron moves between different sites (see Fig. 2). Expressions for t_{eff} and t'_{eff} are given in Eqs. (23), (24) in the supplementary material. We plot their values in Fig. 3, for a wide range of Ω and α_p values.

For a fixed α_p , a smaller Ω implies a larger g/Ω ratio [Eq. (14) in supplementary material], *i.e.* a stronger effective coupling. This explains the smaller $t_{\text{eff}}, t'_{\text{eff}}$ as Ω decreases to be typical polaronic physics: stronger interactions lead to heavier polarons [20]. However, note that these ratios are not exponential in the coupling, like for normal lattice polarons, but rather weakly dependent on the various parameters. This is due to non-linear effects, namely the existence of a maximum allowed value of the induced dipole moment. Both t_{eff}/t and t'_{eff}/t' are around 50% for a wide range of values centered on our

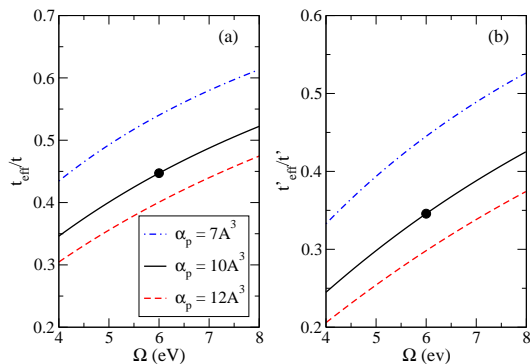


FIG. 3: (a) t_{eff}/t and (b) t'_{eff}/t' vs. Ω , for a polarizability $\alpha_p = 7, 10$ and 12\AA^3 . The dots show the values used here.

parameters, suggesting a light polaron with an effective mass roughly twice as big as the free band carrier.

Such renormalization of the band-structure compared to that predicted by LDA should be detected by ARPES. Interestingly, a recent measurement [21] showed reasonable fits to LDA upon rescaling the bandwidth by a factor of 2.2, similar to our typical values (the material studied has P instead of As, and these smaller anions have a smaller polarizability $\alpha_p \approx 7\text{\AA}^3$). To first order in perturbation theory, we also predict a quasiparticle weight which is independent of \vec{k} , with $Z = 0.38$ for our parameters. The remaining spectral weight should be observed at much high energies typical of the excited As polarization clouds, of the order $\frac{1}{2} \left[\Omega + \sqrt{\Omega^2 + 4g^2} \right] = 5\text{eV}$ and higher (more details are in the supplementary material).

We now study a system with 2 doping electrons, also within first order perturbation in the hopping. We focus on singlet solutions (eigenstates are either singlets or triplets of the two electrons). Also, we first analyze results for $t' = 0$, then investigate the role of a finite t' .

If there were no interactions between the two polarons, then for a total momentum \vec{k} one would get a continuum of eigenstates with energies $E_P(\vec{k} - \vec{q}) + E_P(\vec{q})$ for all \vec{q} in the Brillouin zone, with the ground-state at $\vec{k} = \vec{q} = 0$. However, there are short range interactions between the polarons. If the charges are 2^{nd} nn or closer to each other, some As ions are simultaneously nn to both charges and acquire a dipole moment different from that of As ions which interact with a single charge. This leads to different energies U_0 , U_1 and U_2 for configurations with the two charges being, respectively, on-site, nn and 2^{nd} nn to each other. We sketch below the derivation of U_0 and U_1 . The effective hopping between these configurations is also different from t_{eff} , because of the overlap with these differently polarized clouds. These interaction energies and some of the effective hoppings are summarized in Fig. 4 (expressions and plots for all these quantities are provided in the supplementary material).

An on-site bipolaron also has 4 polarization clouds,

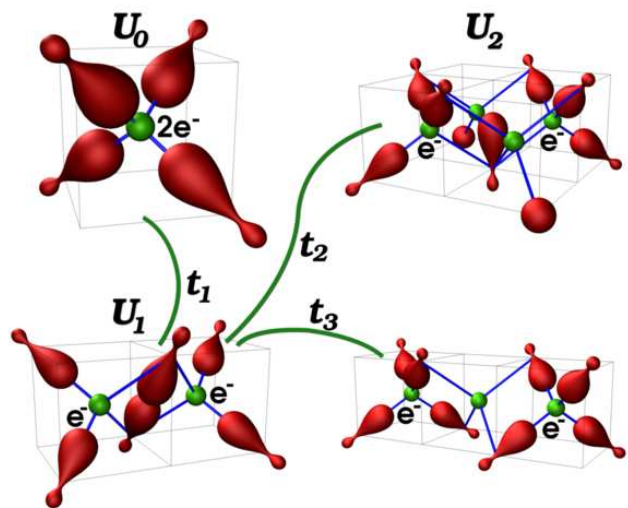


FIG. 4: Sketches of on-site, 1^{st} , 2^{nd} and 3^{rd} nn bipolarons. The first three configurations have interaction energies U_0, U_1 and U_2 , respectively. Several of the special effective hopping integrals are also indicated.

however effectively $g \rightarrow 2g$ in Eq. (3), as the on-site charge is doubled, so its electrostatic energy can be immediately obtained from Eq. (4) to be $E_{BP,0} = U_H + 4(\Omega - \sqrt{\Omega^2 + 16g^2})$. The energy of two static distant polarons is $E_{BP,\infty} = 8(\Omega - \sqrt{\Omega^2 + 16g^2})$, therefore $U_0 = E_{BP,0} - E_{BP,\infty} = U_H - 4 \left[\sqrt{\Omega^2 + 16g^2} + \Omega - 2\sqrt{\Omega^2 + 4g^2} \right] < U_H$ always. This is obvious in the linear regime: because the electric field is twice as large, the energy of the bipolaron is 4 times that of a polaron, *i.e.* twice as large as of two free polarons. This leads to a significant screening of U_H , of several eV, as shown in Fig. 5(a) (these values are smaller than in Ref. 8 because of non-linear effects). Such a strong on-site attraction is well-known to arise for polarons in general [22].

A nn bipolaron has 6 polarization clouds (see Fig. 4), the two central ones being larger than the regular polaron clouds. In the linear regime, the energy of each central cloud is $-\alpha_p(\vec{E}_1 + \vec{E}_2)^2/2$, so the energy difference with respect to two regular clouds is $-\alpha_p\vec{E}_1 \cdot \vec{E}_2 < 0$ if the Fe-As-Fe angle is less than 90° , as is here. This means an attractive nn interaction, as indeed seen for typical parameters in Fig. 5(b). However, because of non-linear effects, this interaction becomes repulsive at strong coupling, as shown in Fig. 5(d). Interestingly, this figure reveals that these materials are close to optimal, with U_1 near its minimum, for typical values of the parameters (see also Fig. 3 in the supplementary material).

This nn attraction *is not* typical polaron physics. On a 2D lattice like in cuprates, the interaction between electronic polarons is *repulsive* because the Cu-O-Cu angle is 180° (the same holds true for polarons coupled to a breathing-mode phonon of the O atoms). For a Holstein

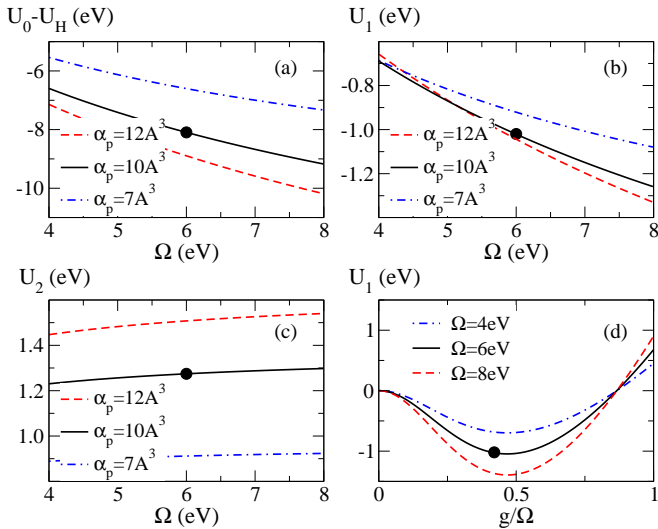


FIG. 5: (a) Renormalization of on-site interaction, $U_0 - U_H$; (b) nn energy U_1 and (c) 2^{nd} nn energy U_2 vs. Ω for various polarizabilities. (d) U_1 vs. g/Ω when $\Omega = 4, 6, 8$ eV. The dots show our typical values.

bipolaron, there is a weak nn attraction, but it is due to spin exchange and is $\mathcal{O}(t^2)$, not $\mathcal{O}(t^0)$ like here [22]. Its non-2D geometry is the essential ingredient in bringing about this strong nn attraction, for the Fe-based superconductors. This mechanism is absent in cuprates.

First order perturbation in hopping mixes these static configurations. Following the calculation described in the supplementary material, we obtain the eigenenergies $E_{BP}(\vec{k})$ for a total momentum \vec{k} . In Fig. 6(a) we plot $\vec{k} = 0$ eigenenergies for all bound bipolaron states, *i.e.* which have energies below the two-polaron continuum starting at $-8t_{\text{eff}}$. We find 3 such states. The GS first shows linear dependence on U_H and then flattens out. Its wavefunction has *s*-type symmetry (unchanged sign upon 90° rotation). There is a second *s*-state at small

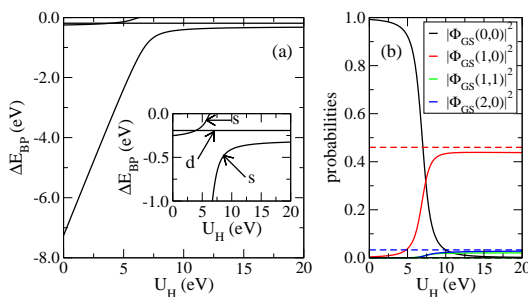


FIG. 6: (a) Eigenstates below the two-polaron continuum, $\Delta E_{BP} = E_{BP}(0) + 8t_{\text{eff}}$ vs. U_H . The symmetry of the three bound eigenstates is labeled in the inset. (b) Probability for on-site, 1^{st} , 2^{nd} and 3^{rd} nn separation in the ground state, vs. U_H . The dashed lines show the same quantities for the *d*-state. We use $t' = 0, \alpha_p = 10\text{\AA}^3, \Omega = 6\text{eV}$ (similar results are found for all $\alpha_p = 7 - 12\text{\AA}^3, \Omega = 4 - 8$ eV).

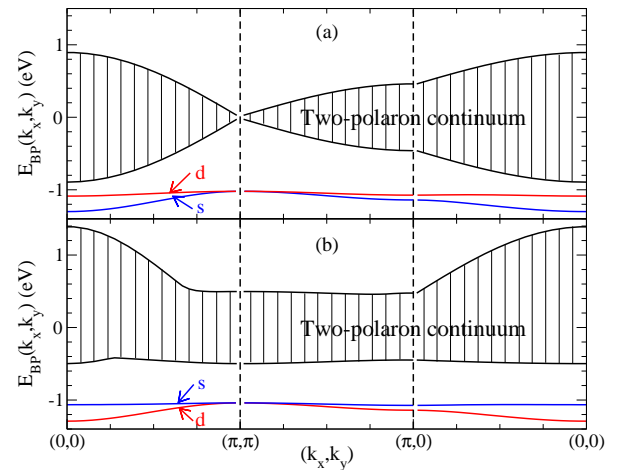


FIG. 7: Dispersion of the two bound bipolaron states along high-symmetry axes in the Brillouin zone, for (a) $t' = 0$ and (b) $t' = -t/2$. The two-polaron continuum is also shown. Parameters are $U_H = 10$ eV, $\alpha_p = 10\text{\AA}^3, \Omega = 6$ eV (similar results are found for all $\alpha_p = 7 - 12\text{\AA}^3, \Omega = 4 - 8$ eV). The symmetry of the ground state changes from *s* to *d* if $t' \neq 0$.

U_H , which then joins the continuum. The 3^{rd} bound bipolaron state has an energy independent of U_H , and is *d*-type (wavefunction changes sign upon 90° rotation).

The nature of these bound states is revealed in Fig. 6(b). For low U_H values, the GS primarily consists of an on-site bipolaron, with hardly any contribution from nn or more distant configuration. This explains why its energy here scales with U_H (more precisely with U_0). When $U_0 \approx 0$ there is a fast crossover to a state dominated by the nn bipolaron configurations (a combined total of 90% probability). This is expected, since $U_1 < 0$ irrespective of U_H , favoring such a pair when U_0 becomes repulsive. The onsite contribution is now exponentially small. This explains the weak U_H dependence here, as coming from virtual hopping to the on-site configuration. The dashed lines show the contributions for the *d*-type state. As expected, it is dominated by nn bipolarons. It has a zero on-site probability, consistent with its symmetry and explaining the lack of dependence on U_H . The 2^{nd} nn contribution is also zero ($U_2 > 0$ as well). There are small 3^{rd} and more distant bipolaron contributions.

The unscreened Hubbard repulsion is very large, $U_H \sim 10 - 20$ eV. For these values there is hardly any dependence on U_H , so its precise value is of little importance. We use $U_H = 10$ eV from now, and ask how mobile are these bound, predominantly nn, bipolaron pairs. Their dispersion in the Brillouin zone is shown in Fig. 7(a), where we also show the two-polaron continuum (eigenstates above the continuum are not shown). The *s*-pair has a bandwidth $E_{GS}(\pi, \pi) - E_{GS}(0, 0) \approx 0.3$ eV, implying a bipolaron mass about 7 times that of a free carrier mass (the bandwidth of a free electron is $8t = 2\text{eV}$). This is not a huge enhancement, since it means that the bipo-

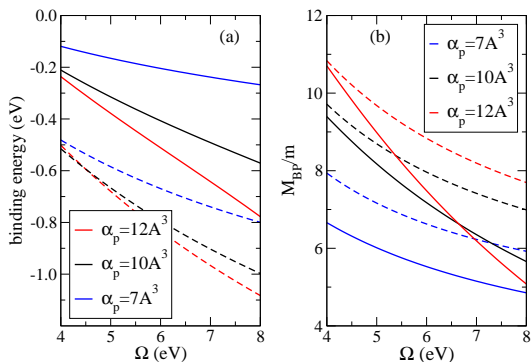


FIG. 8: Ground-state bipolaron (a) binding energy, and (b) effective mass in units of the free carrier mass vs. Ω , for various polarizabilities. The full lines correspond to $t' = 0$, dashed lines to $t' = -t/2$. Here $U_H = 10\text{eV}$.

laron is about 3.5 times heavier than a single polaron. In Fig. 8(b) we plot the bipolaron mass for various α_p and Ω values, showing only limited variation over a wide parameter range. The higher energy d -pair is heavier, with a much narrower bandwidth.

If we include 2^{nd} nn hopping $t' = -t/2$, two effects are apparent. First, the two-polaron continuum is pushed to higher energies, effectively increasing the binding energies of both bound bipolaron states. (The binding energies for the GS bipolaron are shown in Fig. 8(a) for various parameters). Second, the d -state becomes the ground-state. This is not surprising, since the 2^{nd} nn hopping links directly the two nn bipolaron configurations which give the bulk contribution to these eigenstates. Since $t' < 0$, this mixing raises the energy of an s state and lowers that of a d -state. Thus, if the effective t' between the two nn bipolaron configurations is large enough, the d state has to become the ground-state.

Let us now comment briefly on the triplet eigenstates. Since there is no onsite triplet bipolaron configuration, their energies are essentially identical to the energies of the singlet eigenstates in the limit $U_H \rightarrow \infty$. This implies that at this level of approximation and for large enough U_H , singlet and triplet bound bipolarons are almost degenerate. However, it is well known that second-order perturbation theory produces an exchange interaction which strongly favors the singlet eigenstates (this is the interaction responsible for binding the S1 Holstein bipolaron, see for example Ref. 22). It follows that in reality, the ground-state must be a singlet.

The binding energies shown in Fig. 8(a) are substantial, even without inclusion of this singlet exchange energy. As discussed in the supplementary material, relaxation of our approximations (that only As ions nn to a charge are polarized and that dipole-dipole interactions are ignored) further enhances U_1 , and therefore these binding energies, to several eV. Yet more enhancement is expected if we include even higher orbitals than

$5s$ when describing the As ion polarization. All this suggests the appearance of pre-formed pairs well above room temperature. On the other hand, in our model Hamiltonian we have ignored a nn repulsion energy which comes from the bare Coulomb interaction itself (in reality, this nn Coulomb repulsion will be reduced by other screening mechanisms, such as the bond polarizabilities involving the As $4p$ and Fe $3s$ and $4p$ states). This nn repulsion will decrease U_1 substantially, and may even change its sign, making nn bipolaron pairs unstable. It is difficult to obtain accurate quantitative estimates of all these terms, to find out whether bound bipolaron states exist and what are their binding energies.

It is important to point out that the presence of this As-mediated nn attractive interaction U_1 may be essential even if preformed bipolaron pairs do not exist. This would put these materials in a BCS-like framework, with the phonon glue replaced by a virtual excitonic glue. Because U_1 is so large one does not really need much of a retardation effect to overscreen the bare Coulomb repulsion. In favor of this scenario is experimental data indicating higher T_c in samples with shorter Fe-As distances and smaller Fe-As-Fe angles, which is precisely what increases the value of U_1 (more speculation on this is presented in the supplementary material).

However we do not want to rule out the presence of preformed pairs of the kind discussed above. There is ample evidence that singlet pairs could exist to quite high temperatures in these systems. For example, the magnetic susceptibility [23] shows the same strong increase with temperature above the spin density wave (SDW) or superconducting transition temperature. This is very difficult to explain if we start from a free single-particle-like picture, but easy to understand if we assume the presence of singlet preformed pairs well above T_c , with a binding energy of the order of 100meV or more. The magnetic susceptibility of such a system would increase with increasing T with an activated kind of behavior. NMR Knight shift data also displays this kind of behavior [24].

We therefore suggest to take the scenario of preformed singlet bipolarons seriously. We note that a superconducting state would then behave more like a Bose Einstein condensate. At first glance one might think that its T_c would have to be very low, however we note that these bipolarons are very light, with a mass which is about 3-4 times the single polaron mass, and thus very high condensation temperatures could be expected. The other rather interesting aspect to consider is that perhaps this scenario might also explain the low amplitude SDW observed at low dopings, as being a different kind of condensate of singlet bipolarons due to rather strong exchange interactions. The low amplitude would be a result of the pair-wise singlet formation tendency competing with the pair-pair exchange interactions which would favor the SDW. We propose to study these issues next.

Acknowledgments: We thank J. Zaanen, J. van den

Brink, C. Varma, D. Bonn and A. Damascelli for many stimulating discussions and insightful opinions. This work was supported by NSERC, by CIFAR Nanoelectronics and Quantum Materials, and by the Killam Trust and the Alfred P. Sloan Foundation (M.B.).

Competing interests statement: The authors declare no competing financial interests.

-
- [1] Anderson, P. W. More is different. *Science* **177**, 393-396 (1972).
- [2] Bardeen, J., Cooper, L. N., & Schrieffer, J. R. Microscopic Theory of Superconductivity. *Phys. Rev.* **106**, 162 - 164 (1957).
- [3] Kamihara Y. *et al.* Iron-Based Layered Superconductor: LaOF_xP. *J. Am. Chem. Soc.* **128**, 10012 -10013 (2006).
- [4] Kamihara Y. *et al.* Iron-Based Layered Superconductor La[O_{1-x}F_x]FeAs (x = 0.05-0.12) with T_c = 26 K. *J. Am. Chem. Soc.* **130**, 3296 -3297 (2008).
- [5] Takahashi, H. *et al.* Superconductivity at 43 K in an iron-based layered compound LaO_{1-x}F_xFeAs. *Nature* **453**, 376-378 (2008).
- [6] Chen, X. H. *et al.* Superconductivity at 43 K in SmFeAsO_{1-x}F_x. *Nature* **453**, 761-762 (2008).
- [7] Chen, G. F. *et al.* Superconductivity at 41 K and Its Competition with Spin-Density-Wave Instability in Layered CeO_{1-x}F_xFeAs. *Phys. Rev. Lett.* **100**, 247002 (2008).
- [8] Sawatzky, G. A. *et al.* Heavy anion solvation of polarity fluctuations in Pnictides. Preprint at (<http://arxiv.org/abs/0808.1390>) (2008).
- [9] Zhang, F. C. & Rice, T. M. Effective Hamiltonian for the superconducting Cu oxides. *Phys. Rev. B* **37**, 3759 - 3761 (1988).
- [10] Cao, C. *et al.* Proximity of antiferromagnetism and superconductivity in LaO_{1-x}F_xFeAs: effective Hamiltonian from ab initio studies. *Phys. Rev. B* **77**, 220506 (2008).
- [11] Haule, K. *et al.* Correlated electronic structure of LaO_{1-x}F_xFeAs. *Phys. Rev. Lett.* **100**, 226402 (2008).
- [12] Yin, Z. P. *et al.* Electron-hole symmetry and magnetic coupling in antiferromagnetic LaOF_xFeAs. *Phys. Rev. Lett.* **101**, 047001 (2008).
- [13] Si, Q. & Abrahams, E. Strong Correlations and Magnetic Frustration in the High T_c Iron Pnictides. *Phys. Rev. Lett.* **101**, 076401 (2008).
- [14] Xu, C. *et al.* Ising and spin orders in iron-based superconductors. *Phys. Rev. B* **78**, 020501 (2008).
- [15] Chen, W. *et al.* Strong Coupling Theory for Superconducting Iron Pnictides. Preprint at (<http://arxiv.org/abs/0808.3234>) (2008).
- [16] Maier, T. A. & Scalapino, D. J. Theory of neutron scattering as a probe of the superconducting gap in the iron pnictides. *Phys. Rev. B* **78**, 020514(R) (2008).
- [17] Raghun, S. *et al.* Minimal two-band model of the superconducting iron oxypnictides. *Phys. Rev. B* **77**, 220503(R) (2008).
- [18] Lee, P. A. & Wen, X.-G. Spin-triplet p-wave pairing in a 3-orbital model for FeAs superconductors. Preprint at (<http://arxiv.org/abs/0804.1739>) (2008).
- [19] Singh, D. J. & Du, M.-H. Density functional study of LaFeAsO_{1-x}F_x: a low carrier density superconductor near itinerant magnetism. *Phys. Rev. Lett.* **100**, 237003 (2008).
- [20] Goodvin, G. L., Berciu, M. & Sawatzky, G. A. The Green's function of the Holstein polaron, *Phys. Rev. B* **74**, 245104 (2006).
- [21] Lu, D. H. *et al.* Electronic structure of the iron-based superconductor LaOF_xP. *Nature* **455**, 81-84 (2008).
- [22] Macridin, A., Sawatzky, G. A. & Jarrell, M. Two-dimensional Hubbard-Holstein bipolaron. *Phys. Rev. B* **69**, 245111 (2004).
- [23] Klingeler, R. *et al.* Evidence for antiferromagnetic correlations in superconducting LaFeAsO_{1-x}F_x. Preprint at (<http://arxiv.org/abs/0808:0708>) (2008).
- [24] Grafe, H.-J. *et al.* ⁷⁵As NMR studies of superconducting LaO_{0.9}F_{0.1}FeAs. *Phys. Rev. Lett.* **101**, 047003 (2008).

Supplementary material

for the article “*Electronic polarons and bipolarons in Fe-based superconductors: a pairing mechanism*” by Mona Berciu, Ilya Elfimov and George A. Sawatzky.

Contents

I. The model: lattice and Hamiltonian	2
A. Parameters	5
II. The single electronic polaron	8
A. Zero order perturbation: $t = 0$	9
B. First order perturbation	11
III. The bipolaron	13
A. Zero order perturbation: interaction energies	14
B. First order perturbation: effective hopping integrals	19
IV. Estimates for the accuracy of various approximations	25
V. Link between BCS-like theory and experimental data	27
References	29

I. THE MODEL: LATTICE AND HAMILTONIAN

The idealized FeAs layer of interest is sketched in Fig. 1, which shows the cubic lattice (lattice constant $a = 2.8\text{\AA}$) which has the Fe in the center of the cubes, on a simple square lattice. The As are divided equally between the top and bottom layers, as indicated. Each Fe has 4 nearest neighbor As (at a distance $R = a\sqrt{3}/2 = 2.4\text{\AA}$), arranged in a perfect tetrahedron, two in the upper and two in the lower layer. (The real structure has somewhat distorted tetrahedra).

In our model, we assume that the valence electrons occupy $3d$ orbitals of the Fe atoms. We are interested in excess charges on the Fe sites, be they electrons or holes, and we describe them in an effective single band model: we assume that they can hop between nearest neighbor Fe, with a hopping integral t . We will also consider separately the effect of second nearest neighbor hopping, with a hopping integral t' . There is very little hybridization of these $3d$ orbitals with As orbitals, and we ignore it altogether [1]. On-site Hubbard repulsion for these charges, characterized by an energy U_H , is also included. The value of t, t', U_H and of the other parameters introduced below is discussed in the next subsection. Thus, the hopping Hamiltonian for the extra charges on the Fe sites is:

$$\mathcal{H}_{\text{Fe}} = \hat{T} + \hat{T}' + \hat{U} = -t \sum_{\langle i,j \rangle, \sigma} (c_{i,\sigma}^\dagger c_{j,\sigma} + h.c.) - t' \sum_{\langle\langle i,j \rangle\rangle, \sigma} (c_{i,\sigma}^\dagger c_{j,\sigma} + h.c.) + U_H \sum_i \hat{n}_{i\uparrow} \hat{n}_{i\downarrow} \quad (1)$$

where $c_{i,\sigma}^\dagger$ creates an extra charge on the Fe site i with spin σ , $\hat{n}_{i\sigma} = c_{i\sigma}^\dagger c_{i\sigma}$ and $\langle i, j \rangle, \langle\langle i, j \rangle\rangle$ denote summation over the nearest, respectively second nearest neighbor Fe sites. A more detailed model taking in consideration the various relevant $3d$ orbitals is of course possible,

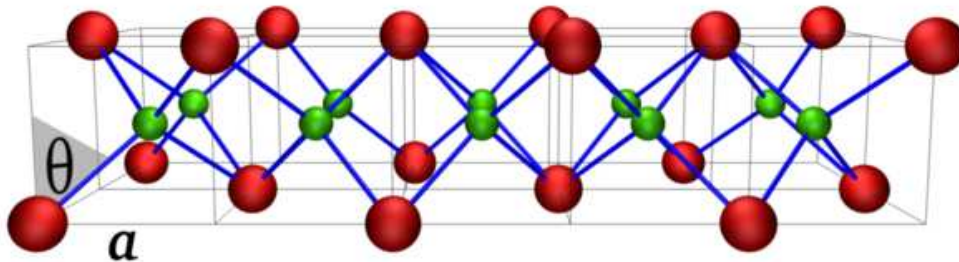


FIG. 1: 3D sketch of the FeAs layer. The lattice constant is a and the angle θ between the Fe-As direction and the z -axis is indicated.

but not necessary for our purposes. We avoid such complications in order to make more transparent the essential new physics proposed in our model.

Ab-initio calculations find that the anions are effectively in the As^{3-} state, with fully occupied $4p$ bands lying well below the Fermi energy [1]. In reality, these As $4p$ states are strongly hybridized with Fe $4s$ and $4p$ orbitals (this hybridization is responsible for the fact that the effective As charge inside the muffin tin is much less than the ionic charge of -3 , [1]). Since this mixing is strongly dependent on the Fe $3d$ occupation, it will provide a screening mechanism for the bare Coulomb repulsion, in particular for the value of U_H . In the following we consider that such screening is already included in U_H . For simplicity, we also refer only to the full As $4p$ orbitals, ignoring their hybridization with the Fe $4s$ and $4p$ orbitals (this could also be accounted for in a multi-band model, but is of limited relevance and we ignore it for clarity).

In our model, the only role of these As ions is that they become polarized due to the electric field created when an extra charge (electron or hole) is on a nearby Fe atom. This is due to transitions of As electrons from the filled $4p$ shell into (primarily) the empty $5s$ shell, and results into a dipole moment (polarization cloud) pointing towards the Fe atom which hosts the extra charge. For simplicity, we only consider the polarization of the 4 As atoms closest to the Fe hosting a charge and we ignore the dipole-dipole interactions between these As polarization clouds. The quantitative importance of these approximations is discussed towards the end of this supplementary material.

Three more observations are in order. First, it is more convenient to describe the As polarization clouds not in terms of an electron being excited from the filled $4p$ orbitals into the empty $5s$ orbital but, equivalently, in terms of a hole being excited from the $5s$ into the $4p$ orbitals. Thus, each As will be described by 4 operators: $s_{\sigma}^{\dagger}, p_{x,\sigma}^{\dagger}, p_{y,\sigma}^{\dagger}, p_{z,\sigma}^{\dagger}$, which create a hole of spin σ in the respective orbital. The ground-state, then, is $s_{\uparrow}^{\dagger}s_{\downarrow}^{\dagger}|0\rangle$ and the p -orbitals lie at an energy Ω above it. If we measure energies above the s -orbital, the Hamiltonian of the unperturbed As ions is:

$$\mathcal{H}_{\text{As}} = \Omega \sum_{i,\lambda,\sigma} p_{i,\lambda,\sigma}^{\dagger} p_{i,\lambda,\sigma} \quad (2)$$

where i is the location of the As atom (see below), $\lambda = x, y, z$ and σ is the spin of the hole.

The second observation is that this Hamiltonian ignores hopping of charges between As atoms. This is a reasonable approximation given the large distance between neighbor As

atoms, which results in rather narrow As bands, as demonstrated by ab-initio calculations. This is why we model the As within this rather atomistic picture.

Finally, the lattice illustrated in Fig. 1 suggests that we should consider a unit cell with (a minimum of) 2 Fe atoms and 2 As atoms, one in the top and one in the bottom layer. However, given our assumptions, in our model it makes no difference whether half the As are above and half are below the Fe layer, or whether they are all in the same plane (for example, in the layer below the plane of Fe). Mathematically, this follows because for the As in the layer above, one can redefine the p_z operators as $p_z \rightarrow -p_z$, which is equivalent to a local flipping of the direction of the z -axis. This is very convenient, since it allows us to use a simple unit cell with one Fe and one As in the basis, as illustrated schematically in Fig. 2. However, it is important to point out that if one wants to include, for example, As dipole-dipole interactions, than one needs to carefully consider the true orientations of the As polarization clouds with respect to one another.

Figure 2 also indicates our choice for indexing the lattice sites, with Fe_i and As_i being the unit cell of the simple square lattice. If the charge is on Fe_i , the polarization of As_i and the other 3 As neighbors is pointing in its direction. It is therefore more convenient to use the 1, 2 axes orientation for the in-plane directions (see Fig. 2), and 3 = z for the out-of-plane direction, in terms of which $p_1 = \frac{1}{\sqrt{2}}(p_x - p_y)$, $p_2 = \frac{1}{\sqrt{2}}(p_x + p_y)$, $p_3 = p_z$ and \mathcal{H}_{AS} remains formally identical to that of Eq. (2), except that now $\lambda = 1, 2, 3$.

With these definitions, the cloud of As_i is pointing towards Fe_i in the direction $-\sin \theta \vec{e}_2 + \cos \theta \vec{e}_3$, where $\cos \theta = \frac{1}{\sqrt{3}}$ comes from simple geometry illustrated in Fig. 1. Of course, Fe_i also interacts with As_{i-x} , As_{i-x-y} and As_{i-y} . Their polarization vectors are obtained by appropriate rotations from the one just listed.

The interaction Hamiltonian is, then:

$$\begin{aligned} \mathcal{H}_{\text{int}} = g \sum_{i,\sigma} \hat{n}_i & \left[s_{i,\sigma}^\dagger (-\sin \theta p_{i,2,\sigma} + \cos \theta p_{i,3,\sigma}) + s_{i-x,\sigma}^\dagger (\sin \theta p_{i-x,1,\sigma} + \cos \theta p_{i-x,3,\sigma}) \right. \\ & \left. + s_{i-x-y,\sigma}^\dagger (\sin \theta p_{i-x-y,2,\sigma} + \cos \theta p_{i-x-y,3,\sigma}) + s_{i-y,\sigma}^\dagger (-\sin \theta p_{i-y,1,\sigma} + \cos \theta p_{i-y,3,\sigma}) + h.c. \right] \end{aligned} \quad (3)$$

where the sum is over all unit cells i in the lattice. This interaction describes the $s \rightarrow p$ transitions and resulting polarization of the As clouds (with the appropriate orientations) if extra charges, counted by $\hat{n}_i = \hat{n}_{i\uparrow} + \hat{n}_{i\downarrow}$, are on Fe_i site.

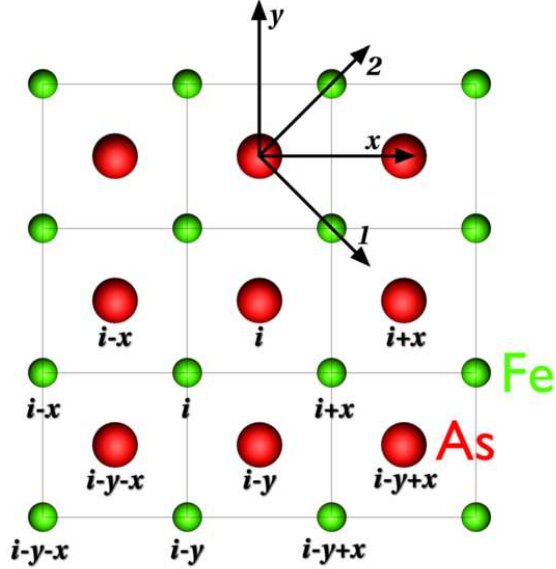


FIG. 2: Top view of the Fe-As structure. Several sites are indexed. The orientations of the in-plane axes 1,2 and x, y is also indicated. The Fe and As layers have different depths in the z direction.

Our model Hamiltonian $\mathcal{H} = \mathcal{H}_{\text{Fe}} + \mathcal{H}_{\text{As}} + \mathcal{H}_{\text{int}}$ is thus characterized by 5 parameters, t, t', U_H, Ω, g . We now discuss the choice of their values.

A. Parameters

Ab-initio calculations find the Fe $3d$ dispersive part of the bandwidth to be roughly $W = 2eV$ [1]. Our 2D hopping model has a bandwidth $W = 8t$ irrespective of the value of t' , thus $t = 0.25eV$ is a typical value. For t' , we will consider both the case $t' = 0$ and $t' = -t/2 = -0.125eV$, which is the appropriate value for hopping between d_{xy} and the like orbitals which contribute most near the Fermi level. The Hubbard repulsion U_H is certainly a large energy. We will use it as a parameter, and show that our results are very weakly sensitive to its precise value once $U_H > 8 eV$ or so, which is certain to be the case.

The ab-initio calculations also suggest a difference from the top of the As $4p$ bands to the bottom of the As $5s$ bands of about $4eV$. This value provides a lower limit for the split Ω between the s and p orbitals. A more appropriate measure would be the distance between the mid-points of these bands, but this is harder to estimate. We use $\Omega = 6eV$ as a typical value, and also study the effects of larger Ω values on the results. This is also reasonable

because higher-energy orbitals of the As will be polarized as well, so one can think of these s and p orbitals as modeling effectively the polarization of the whole atom.

The final parameter needed is g . Since this characterizes the $s - p$ hybridization when an As polarization cloud is created, we should extract it from the As polarizability α_p . Its value is not known precisely, but the polarizability is typically equal to the volume of the atom. Since As is a big atom, its polarizability is estimated to be $\alpha_p = 10 - 12 \text{\AA}^3$.

Consider the polarization cloud formed on an As ion, due to a charge q placed at a distance R away, in the direction characterized by the versor \vec{e} . The electric field at the As site is then $\vec{E} = \frac{q}{R^2} \vec{e}$. Note that we use an unscreened value for this electric field. The reason is that we are interested in behavior related to the high-frequency dynamic electronic polarizability, and not that due to slow vibrational motion of the As themselves. As we show below, the effective masses of the polarons and bipolarons are fairly small, meaning that they are highly mobile. The As ions are fast to acquire a polarization cloud, but since they are very heavy, they simply cannot move fast enough to follow the fast polaron dynamic. This separation of energy scales allows us to ignore lattice dynamics effects in the following. The interaction between the As and the electric field is $\mathcal{H}_{\text{int}} = -\hat{p} \cdot \vec{E}$, where \hat{p} is the As dipole moment operator. In the second quantization, and if we restrict ourselves only to s and p orbitals to describe the As, its dipole moment is

$$\hat{p} = \sum_{\lambda, \sigma} \langle s | e \vec{r} | p_\lambda \rangle \left(s_\sigma^\dagger p_{\lambda, \sigma} + h.c. \right) \quad (4)$$

where $\lambda = x, y, z$ or $\lambda = 1, 2, 3$ (either basis is equivalent), and we already took in consideration the fact that there are no matrix elements of the dipole moment between orbitals of the same level ($\langle s | \vec{r} | s \rangle = 0$, etc). Moreover, $\langle s | e \vec{r} | p_\lambda \rangle = e \vec{e}_\lambda a_{\text{As}}$, since the operator \vec{r} has a non-vanishing matrix element only in the direction \vec{e}_λ of the orbital p_λ involved. Thus, a_{As} is a characteristic “size” of the ion, defined as:

$$a_{\text{As}} = \langle s | x | p_x \rangle = \int d\vec{r} \phi_x^*(\vec{r}) x \phi_{p_x}(\vec{r}) = \langle s | y | p_y \rangle = \langle s | z | p_z \rangle \quad (5)$$

In terms of this, we find:

$$\mathcal{H}_{\text{int}} = -\frac{e a_{\text{As}} q}{R^2} \sum_{\lambda, \sigma} \left(\vec{e} \cdot \vec{e}_\lambda s_\sigma^\dagger p_{\lambda, \sigma} + h.c. \right) \quad (6)$$

This is exactly the form used in Eq. (3), except there we have explicitly written the various projections $\vec{e} \cdot \vec{e}_\lambda$ in terms of the angle θ appropriate for our geometry. It follows that

$g = -ea_{\text{As}}q/R^2$. As we show in the following, the energetics only depends on g^2 , i.e. it is the same for both electron or hole extra charges on the Fe atom. Since the sign of g is irrelevant, from now on we assume that the extra charges are electrons, $q = -e$, so that:

$$g = \frac{a_{\text{As}}e^2}{R^2} > 0. \quad (7)$$

This shows that g is an energy equal to the typical induced dipole ea_{As} times the applied electric field e/R^2 .

For simplicity, in the rest of this discussion let us denote $p_\sigma = \sum_\lambda \vec{e} \cdot \vec{e}_\lambda p_{\lambda,\sigma}$, i.e. it is the annihilation operator for the p orbital oriented in the direction \vec{e} of the applied electric field. Of course, one can form two other linear combinations of the p_x, p_y, p_z orbitals which are orthogonal to this direction. These two do not couple to the electric field and do not participate in the polarization cloud, thus their energetics is trivial. The interesting part for the problem of the As cloud in the presence of the extra charge is therefore described by the Hamiltonian:

$$\hat{h} = \Omega \sum_\sigma p_\sigma^\dagger p_\sigma + g \sum_\sigma (s_\sigma^\dagger p_\sigma + h.c.) \quad (8)$$

This Hamiltonian is trivial to diagonalize. Its ground state has the energy

$$E_{\text{cloud}} = \Omega - \sqrt{\Omega^2 + 4g^2} \quad (9)$$

and the eigenstate

$$|GS\rangle = \gamma_\uparrow^\dagger \gamma_\downarrow^\dagger |0\rangle \quad (10)$$

where

$$\gamma_\sigma^\dagger = \cos \alpha s_\sigma^\dagger - \sin \alpha p_\sigma^\dagger \quad (11)$$

and

$$\begin{aligned} \cos \alpha &= \sqrt{\frac{1}{2} \left(1 + \frac{\Omega}{\sqrt{\Omega^2 + 4g^2}} \right)} \\ \sin \alpha &= \sqrt{\frac{1}{2} \left(1 - \frac{\Omega}{\sqrt{\Omega^2 + 4g^2}} \right)} \end{aligned} \quad (12)$$

Indeed, note that if $g = 0$ this is reduced to the As ground state (holes in the s orbitals, $\alpha = 0^\circ$) whereas for $g \rightarrow \infty$, the γ operators describe the maximally polarized linear combination $(s - p_x)/\sqrt{2}$ and $\alpha = 45^\circ$.

The second eigenstate of \hat{h} has an energy $E_{\text{exc}} = \Omega + \sqrt{\Omega^2 + 4g^2}$ and corresponds to filling up the orbitals $\eta_\sigma^\dagger = \sin \alpha s_\sigma^\dagger + \cos \alpha p_\sigma^\dagger$, i.e. of creating a polarization cloud oriented antiparallel to the electric field. As already discussed, one can also excite the electron in the p orbitals orthogonal to the direction of the electric field, the energy of those states being simply Ω . Given that Ω is a large energy, all these excited states are well above the ground state and will be ignored in the rest of the calculation.

Finally, the dipole moment induced on the As atom is:

$$\langle p \rangle = \langle GS | \vec{e} \cdot \hat{\vec{p}} | GS \rangle = 4ea_{\text{As}} \sin \alpha \cos \alpha = \frac{4ea_{\text{As}}g}{\sqrt{\Omega^2 + 4g^2}} \quad (13)$$

Remember that Eq. (7) revealed that g is proportional to the applied electric field $E = e/R^2$.

This shows that in the limit $g \ll \Omega$ we can approximate

$$\langle p \rangle \approx \frac{4ea_{\text{As}}g}{\Omega} = \frac{4e^2a_{\text{As}}^2}{\Omega} E$$

and thus identify the polarizability from this linear regime where $\langle p \rangle = \alpha_p E$. This allows us to extract a_{As} in terms of α_p and then, through Eq. (7), to calculate:

$$g^2 = \frac{\alpha_p \Omega e^2}{4R^4} \quad (14)$$

Using $\alpha_p = 10\text{\AA}^3$ and $\Omega = 6\text{eV}$ gives the estimate $g = 2.5\text{eV}$ and thus $g/\Omega = 0.4$, suggesting that non-linear effects described by our model are starting to become important, however they are not dominant yet. For example, with these numbers, the energy of the polarized As cloud from Eq. (9) is $E_{\text{cloud}} = -1.78\text{eV}$, whereas in the linear regime $g/\Omega \ll 1$ we would have $E_{\text{cloud}} \approx -\frac{2g^2}{\Omega} = -2.05\text{eV}$. As a consistency check, also note that the linear expression for the energy of the cloud can be rewritten as $E_{\text{cloud}} \approx -\frac{2g^2}{\Omega} = -\frac{\alpha_p E^2}{2}$, as expected to be the case in this regime.

To conclude, we will use $t = 0.25\text{eV}$, $t' = 0$ or -0.125eV , $\Omega = 6\text{eV}$ and $g = 2.5\text{eV}$ as typical numbers. As discussed previously, we will also allow Ω to vary and we will then choose g according to Eq. (14), so that the polarizability stays constant. The corresponding g/Ω ratio is shown in Fig. 3: for a wide range of values of Ω , g/Ω is roughly 0.4-0.5.

II. THE SINGLE ELECTRONIC POLARON

We would like to find the eigenstates of the total Hamiltonian $\mathcal{H} = \mathcal{H}_{\text{Fe}} + \mathcal{H}_{\text{As}} + \mathcal{H}_{\text{int}}$ in the case when there is a single extra charge at one of the Fe sites. Of course, this charge

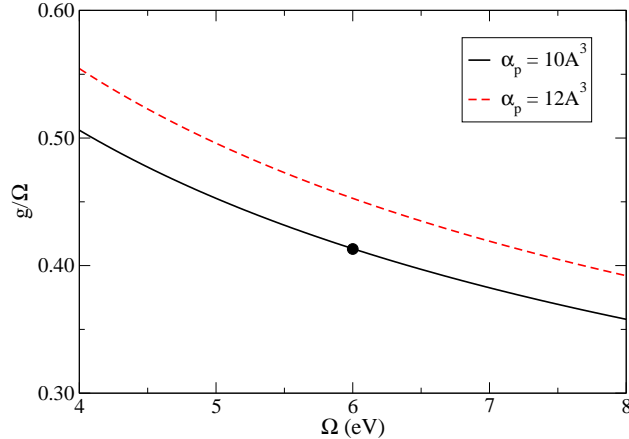


FIG. 3: Ratio g/Ω vs. Ω , for a fixed polarizability $\alpha_p = 10 \text{ \AA}^3$ (full line) and 12 \AA^3 (dashed line). The dot indicates our typical choice of parameters.

can hop around and will also polarize the As atoms in its vicinity. We call this composite object (the charge dressed by the surrounding polarization clouds) an electronic polaron.

To find its low-energy spectrum, we will use perturbation theory in the hopping Hamiltonian. The reason this is a valid approach is that t is by far the smallest energy scale in this problem. A more detailed justification is provided below.

A. Zero order perturbation: $t = 0$

In the absence of hopping the electron will always stay on the same site, say at Fe_i , and will polarize its 4 neighbor As. Since we ignore dipole-dipole interactions in our model, this simply leads to the appearance of 4 polarization clouds like the one discussed in the previous section, each pointing towards the Fe atom. This is illustrated in Fig. 3.

The ground-state energy of the static polaron is then, immediately:

$$E_{P,GS} = 4E_{\text{cloud}} = 4 \left(\Omega - \sqrt{\Omega^2 + 4g^2} \right). \quad (15)$$

The lowest excited state is at an energy $\frac{1}{2} \left[\Omega + \sqrt{\Omega^2 + 4g^2} \right]$ above $E_{P,GS}$, and has either the spin-up or spin-down hole of one of the As atoms polarized in a direction perpendicular to its local electric field. These excited states will be ignored in the following, since $t \ll \Omega$.

To characterize the polarization clouds, we introduce the following operators [analogs of Eq. (11) for the specific geometry here]:

$$\gamma_{i,\lambda,\pm,\sigma}^\dagger = \cos \alpha s_{i,\sigma}^\dagger - \sin \alpha \left(\pm \sin \theta p_{i,\lambda,\sigma}^\dagger + \cos \theta p_{i,3,\sigma}^\dagger \right) \quad (16)$$

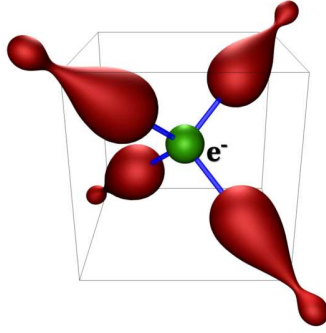


FIG. 4: Pictorial illustration of a static electronic polaron. The electron residing on the central Fe atom polarizes the holes on the nn As sites into the $4p$ orbital pointing towards the Fe. More distant As are assumed to be in the $5s$ ground-state.

where here $\lambda = 1, 2$ shows if the in-plane component of the polarization cloud is oriented along axis 1 or axis 2, and the \pm sign indicates whether the in-plane polarization is parallel or antiparallel to this axis. The angles α and θ were defined in the previous sections.

In terms of these, the ground-state of the system with the electron at site Fe_i is:

$$|\Phi_i\rangle = c_i^\dagger |i\rangle \quad (17)$$

where $|i\rangle$ describes the state of all As atoms when the electron is at site Fe_i (since there is a single such electron, its spin is irrelevant and we drop its index here). Following our discussion in the previous section, we have

$$|i\rangle = \prod_{\sigma} \gamma_{i,2,-,\sigma}^\dagger \gamma_{i-x,1,+,\sigma}^\dagger \gamma_{i-x-y,2,+,\sigma}^\dagger \gamma_{i-y,1,-,\sigma}^\dagger |GS\rangle_i \quad (18)$$

where

$$|GS\rangle_i = \prod_{|j-i|>R,\sigma} s_{j,\sigma}^\dagger |0\rangle, \quad (19)$$

i.e. it describes unpolarized (ground-state) As atoms at all sites which are not nearest neighbor to the site Fe_i containing the extra charge. Thus, the product of γ operators describes the polarization clouds on the 4 neighbor As sites (both spin-up and spin-down holes are polarized), and $|GS\rangle_i$ describes the remaining holes on the unpolarized As sites. Of course, this ground-state $|\Phi_i\rangle$ is highly degenerate since the electron can be at any Fe site. The hopping t lifts this degeneracy.

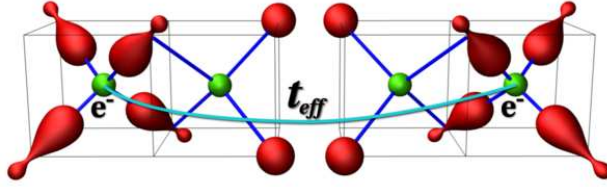


FIG. 5: Single polaron hopping in the x -direction. The hopping integral is renormalized by the overlap between the polarization clouds in the initial and the final position. The unpolarized As atoms are in their ground-state s -orbital.

B. First order perturbation

In the subspace generated by all the ground-states $|\Phi_i\rangle$ described in the previous section, we can form eigenstates which are invariant to translations in the usual fashion:

$$|\Phi_{\vec{k}}\rangle = \sum_i \frac{e^{i\vec{k}\cdot\vec{R}_i}}{N} |\Phi_i\rangle \quad (20)$$

where the lattice has $N \times N = N^2$ unit cells and we assume periodic boundary conditions. As usual, the quasi-momenta \vec{k} are defined inside the first Brillouin zone of the simple square lattice $-\frac{\pi}{a} < k_x, k_y \leq \frac{\pi}{a}$.

Since the hopping Hamiltonian is diagonal in this basis, $\langle\Phi_{\vec{k}}|\hat{T}_{\text{tot}}|\Phi_{\vec{k}'}\rangle \propto \delta_{\vec{k},\vec{k}'}$, it follows that $|\Phi_{\vec{k}}\rangle$ are the eigenstates in first-order perturbation theory. Their energies are:

$$E_P(\vec{k}) = E_{P,GS} + \langle\Phi_{\vec{k}}|\hat{T}_{\text{tot}}|\Phi_{\vec{k}}\rangle \quad (21)$$

with the second term describing the polaron dispersion. Straightforward calculation reveals that:

$$E_P(\vec{k}) = E_{P,GS} - 2t_{\text{eff}} [\cos(k_x a) + \cos(k_y a)] - 4t'_{\text{eff}} \cos(k_x a) \cos(k_y a) = E_{P,GS} + \epsilon_{\text{eff}}(\vec{k}), \quad (22)$$

in other words the dispersion is identical to that of a free particle, but with renormalized hopping integrals (or mass). The renormalization is due to the overlap of the corresponding As clouds as the electron moves from one site to a nearest or second-nearest neighbor site, as illustrated schematically in Fig. 5 for the former case. These overlaps result in:

$$t_{\text{eff}} = t\langle i|i+x\rangle = t \left[\frac{1}{6} \left(1 + \frac{\Omega}{\sqrt{\Omega^2 + 4g^2}} \right) \left(2 + \frac{\Omega}{\sqrt{\Omega^2 + 4g^2}} \right) \right]^4 \quad (23)$$

$$t'_{\text{eff}} = t' \langle i | i + x + y \rangle = t' \left[\frac{1}{2} \left(1 + \frac{\Omega}{\sqrt{\Omega^2 + 4g^2}} \right) \right]^6 \left[\frac{1}{3} \left(1 + \frac{2\Omega}{\sqrt{\Omega^2 + 4g^2}} \right) \right]^2 \quad (24)$$

The results are plotted (in units of bare t , respectively t') in Fig. 6, vs. Ω , for the two values of polarizability $\alpha_p = 10$ and 12\AA^3 . As expected, in the limit of large Ω , which implies $g/\Omega \rightarrow 0$, the ratios increase towards unity because the polarization clouds become very small. As Ω decreases, the effective coupling g/Ω increases and the ratios (and therefore the bandwidths) decrease. This is typical polaronic behavior, however note that even if we are in the strong coupling limit $g/\Omega \rightarrow \infty$, the effective hopping is lowered to at most $t_{\text{eff}}/t = 1/3^4 = 0.012$, $t'_{\text{eff}}/t' = 1/(2^6 3^2) = 0.0017$. While these are, of course, small values, the renormalized hoppings are not becoming exponentially small with increased coupling, as is the case for polarons with phonon clouds. The reason is that within this model, the polarization clouds saturate to a maximum possible value and therefore the overlap cannot become arbitrarily small.

The effective polaron mass renormalization is inversely proportional to the t_{eff}/t ratio (this statement is true if $t' = 0$. If t' is finite both ratios determine the new effective mass, however they are roughly equal). Thus, these polarons remain rather light objects, with a mass up to a factor of 3 or less larger than the bare band mass, if Ω is not too small. The dots in Fig. 6 indicate our chosen values, for which the polaron mass is roughly 2.2 times the mass of the free band electron, and $t_{\text{eff}} = 0.45 \times t \approx 0.11\text{eV}$.

While not huge, this renormalization of the effective hoppings/mass is important since it further supports our use of the perturbation theory. First order perturbation is reasonable

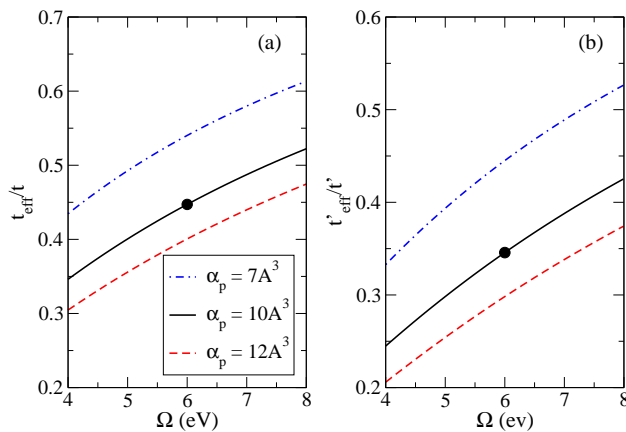


FIG. 6: t_{eff}/t (left) and t'_{eff}/t' (right) vs. Ω , for different As polarizabilities. The dots indicate the main values used here.

only assuming that half the effective bandwidth is much smaller than the distance to the next set of excited states, which were ignored in this calculation. As already discussed, those excited states are at $\frac{1}{2} [\Omega + \sqrt{\Omega^2 + 4g^2}] \approx 5\text{eV}$ and higher energies, whereas $4t_{\text{eff}} \approx 0.45\text{eV}$. These numbers suggest that first order perturbation theory should be quite accurate for parameters in the regime of interest to us (the higher the Ω value used, the more accurate the perturbation theory is). A second order calculation (which is possible, but rather involved) should only bring in relatively small corrections. Moreover, those corrections may well be of the same order as other ignored small terms (like dipole-dipole interactions between the As clouds) and therefore one would need to reconsider all these approximations carefully before going to a higher order in perturbation theory.

In conclusion, our calculation shows that, to first order, the only effect of the formation of the electronic polarons is to scale down the hopping energy scales by a factor of around 2.5 (with slight differences for nearest vs. 2nd nearest neighbor hopping), but otherwise the dispersion is similar to that predicted by LDA for a free charge. ARPES measurements indicating precisely such behavior (in LaOFeP) have been reported already in Ref. 2. In our theory, ARPES would measure a quasiparticle peak at low energies, with a quasiparticle weight

$$Z = |\langle \Phi_{\vec{k}} | c_{\vec{k}}^\dagger | GS \rangle|^2 = [\cos \alpha]^{16} \quad (25)$$

which is independent of momentum (second and higher order corrections to the wavefunctions may bring in some small momentum dependence). For our typical values, this implies $Z = 0.38$. The remaining spectral weight should be observed at much high energies typical of the excited cloud states, of the order $\frac{1}{2} [\Omega + \sqrt{\Omega^2 + 4g^2}] = 5\text{eV}$ or more.

III. THE BIPOLARON

Within the same model and with the same approximations (first-order perturbation theory) we will now calculate the eigenstates of the system when 2 charges are present on the Fe sublattice. In particular, we are interested to see whether they become bound into a so-called bipolaron, or a state of two free polarons is energetically more favorable.

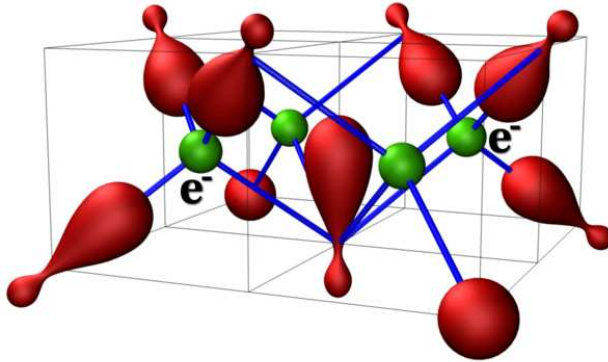


FIG. 7: Polarization clouds for a 2nd nearest neighbor electronic bipolaron. The central “shared” As atom has a polarization different from that of the usual polaron clouds.

A. Zero order perturbation: interaction energies

All the eigenstates of the two charges must be either a singlet or a triplet in the spin space. Since we expect a singlet to be the ground-state (this expectation is verified by our calculations) we focus on calculations for singlet eigenstates. Most of the calculations for triplets are very similar, therefore we will only point out where there are major differences between the two cases.

For convenience, we introduce a singlet creation operator, defined as:

$$s_{i,j}^\dagger = \begin{cases} \frac{1}{\sqrt{2}} (c_{i\uparrow}^\dagger c_{j\downarrow}^\dagger - c_{i\downarrow}^\dagger c_{j\uparrow}^\dagger) & , \text{ if } i \neq j, \\ c_{i\uparrow}^\dagger c_{i\downarrow}^\dagger & , \text{ if } i = j. \end{cases} \quad (26)$$

Within zero-order perturbation theory ($t = 0$) the charges cannot move, being pinned at their initial locations. Depending on the distance between them, different types of polarization clouds can form with different energies. We will now calculate these energies.

If the two electrons are 3rd nearest neighbors or further apart, $|i - j| \geq 2a$, then their polarization clouds do not overlap (there is no As atom that is a nearest neighbor for both of the charged Fe sites). Therefore each charge forms the same 4 clouds as described for single polarons, and the energy is twice the energy of a polaron:

$$E_{BP,\infty} = 2 \times E_{P,GS} = 8 \left[\Omega - \sqrt{\Omega^2 + 4g^2} \right] \quad (27)$$

If the electrons are 2nd nearest neighbors, they share one As atom, as shown in Fig. 7, so only 7 polarization clouds are formed. Six of these are precisely like the ones discussed

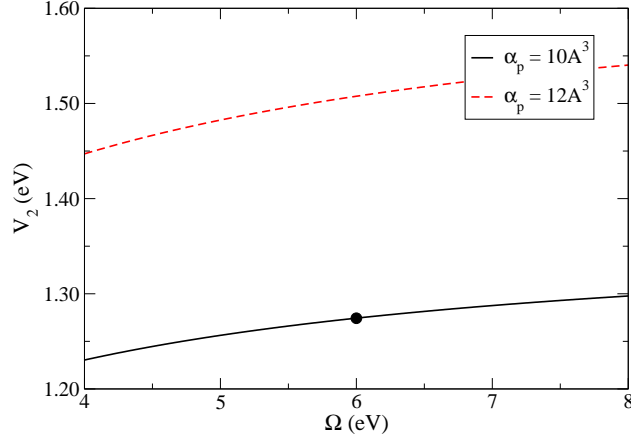


FIG. 8: U_2 vs Ω , for two values of the polarizability. Because $U_2 > 0$ everywhere, it follows that it is energetically more favorable for electrons to stay at distances $|i - j| > 2$ than to be second nearest-neighbors. The dot indicates our typical value.

previously, since each of those As atoms is in the field created by a single charge. The cloud on the central As atom, however, is different, since it is created by the sum of the electric fields from the two charges. Given the geometry of the system, this new cloud is polarized along the z -axis, and this z -axis polarization is twice as big because two charges contribute to it. Thus, the only change in calculating the energy and eigenstate of this cloud is to replace $g \rightarrow 2g \cos \theta = 2g/\sqrt{3}$ in Eq. (8), and of course the generic p orbital is now the $p_z = p_3$ orbital. As result, the energy of this cloud is changed to $\Omega - \sqrt{\Omega^2 + \frac{16}{3}g^2}$ and therefore the total energy of the 2nd nearest neighbor static bipolaron is:

$$E_{BP,2} = 6 \left[\Omega - \sqrt{\Omega^2 + 4g^2} \right] + \left[\Omega - \sqrt{\Omega^2 + \frac{16}{3}g^2} \right] \quad (28)$$

This energy is different from the energy of two free polarons by an amount

$$U_2 = E_{BP,2} - E_{BP,\infty} = 2\sqrt{\Omega^2 + 4g^2} - \Omega - \sqrt{\Omega^2 + \frac{16}{3}g^2} \quad (29)$$

This is plotted in Fig. 8 as a function of Ω , for the two values of As polarizability. In both cases, it is positive and a slowly varying function of Ω . The 2nd nearest neighbor effective interaction is repulsive because the new cloud, although bigger than a single original cloud, is not bigger than two such clouds. As a result, it is energetically more favorable to have two free electronic polarons situated far apart, than to have a second nearest-neighbor bipolaron. This can be shown to be true for any value of the polarizability and of Ω (*i.e* any g/Ω ratio), for this lattice structure.

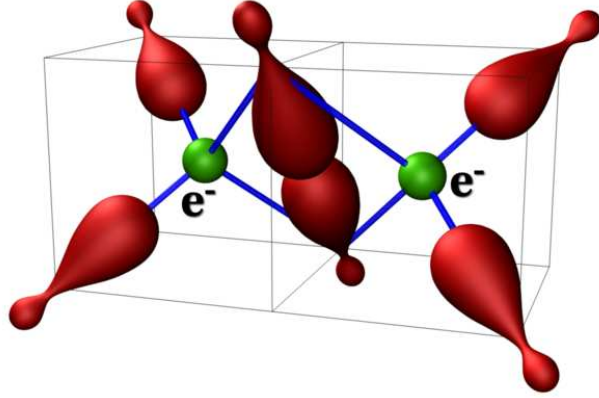


FIG. 9: Polarization clouds for a nearest neighbor electronic bipolaron. The two central “shared” As atoms have a polarization different from that of the usual polaron clouds.

Interestingly, this interaction can be made attractive by changing the lattice structure. Focusing on the weak-coupling regime of small $\frac{g}{\Omega}$ and using a linear approximation, the energy of the new cloud is $\Omega - \sqrt{\Omega^2 + 16g^2 \cos^2 \theta} \approx -8 \cos^2 \theta g^2 / \Omega$, while the energy of two of the original clouds is $\approx -4g^2 / \Omega$. The 2nd nearest neighbor pair becomes energetically favorable when $2 \cos^2 \theta > 1 \rightarrow \theta < 45^\circ$. This can be achieved by making the lattice tetragonal, *i.e.* by increasing the distance between the Fe and As layers by a factor of $\sqrt{2}$ or more. Of course, this would also have the effect of decreasing all the polarization energies, since the electric fields would be smaller due to the increased Fe-As distances

The ground-state eigenstate of this new cloud can be obtained from the general formula, after performing the substitutions discussed above. This leads to the appearance of a new mixing angle:

$$\begin{aligned} \cos \beta &= \sqrt{\frac{1}{2} \left(1 + \frac{\Omega}{\sqrt{\Omega^2 + \frac{16}{3} g^2}} \right)} \\ \sin \beta &= \sqrt{\frac{1}{2} \left(1 - \frac{\Omega}{\sqrt{\Omega^2 + \frac{16}{3} g^2}} \right)} \end{aligned} \quad (30)$$

which appears in the definition of the new cloud. For instance, assuming that this new cloud appears at As_i site, then its creation operator for a given spin is:

$$\tilde{\gamma}_{i,\sigma}^\dagger = \cos \beta s_{i,\sigma}^\dagger - \sin \beta p_{i,3,\sigma}^\dagger \quad (31)$$

A similar analysis applies for a nearest neighbor bipolaron. In this case, as illustrated in Fig. 9, a total of 6 As atoms are polarized. Four of them have clouds of the original type,

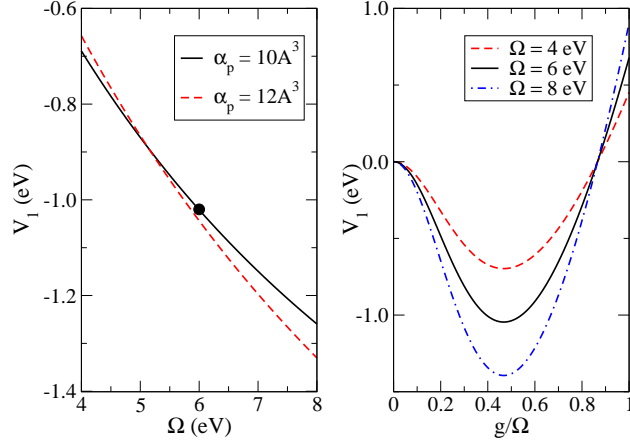


FIG. 10: Left panel: Effective nearest neighbor bipolaron interaction U_1 as a function of Ω for two polarizability values. Right panel: U_1 vs. g/Ω for $\Omega = 4, 6$ and 8 eV.

while 2, which are neighbors to both Fe atoms, have yet another type of polarization cloud which lies in the plane perpendicular to be bipolaron axis. Straightforward geometry shows that this polarization cloud has magnitude $\sqrt{\frac{8}{3}}$ larger than an original cloud, therefore one has to replace $g \rightarrow g\sqrt{\frac{8}{3}}$ (or $4g^2 \rightarrow \frac{32}{3}g^2$) to find the energy of each new cloud.

Thus, the total energy of a static nearest neighbor bipolaron is:

$$E_{BP,1} = 4 \left[\Omega - \sqrt{\Omega^2 + 4g^2} \right] + 2 \left[\Omega - \sqrt{\Omega^2 + \frac{32}{3}g^2} \right] \quad (32)$$

and the difference between this and the energy of two unbound polarons is:

$$U_1 = E_{BP,1} - E_{BP,\text{inf}} = 4\sqrt{\Omega^2 + 4g^2} - 2\Omega - 2\sqrt{\Omega^2 + \frac{32}{3}g^2} \quad (33)$$

This effective energy is plotted in Fig. 10 both as a function of Ω for a fixed polarizability (left panel) and as a function of g/Ω (right panel) for several values of Ω .

The first interesting observation is that this effective interaction is attractive, favoring a bound nearest neighbor bipolaron over two independent polarons. As shown in the right panel, this is only true for small $g/\Omega < 1$ values (if g/Ω becomes large enough, the clouds saturate to their maximum allowed values and the two new clouds are energetically less favorable than four original clouds). Remarkably, the strongest binding energy is for $g/\Omega \approx 0.45$ for reasonable values of Ω , which is close to the values we expect for this parameter (see Fig. 3). From this point of view, we can say that these lattices are already very close to being fully optimized. As discussed for the case of the 2nd nn bipolaron, it is possible

to further change this interaction by changing the lattice geometry: a smaller θ angle will again increase this binding energy, but this is balanced by a decrease if the Fe-As distance is increased.

The creation operators for these new clouds are:

$$\tilde{\gamma}_{i,\pm,\sigma}^\dagger = \cos \gamma s_{i,\sigma}^\dagger - \sin \gamma \frac{\pm p_{i,\lambda,\sigma}^\dagger + p_{i,3,\sigma}^\dagger}{\sqrt{2}} \quad (34)$$

where $\lambda = x$ or y is the direction perpendicular to the bipolaron axis, and the \pm sign shows whether the cloud is parallel/antiparallel to the λ axis. The new mixing angles are:

$$\begin{aligned} \cos \gamma &= \sqrt{\frac{1}{2} \left(1 + \frac{\Omega}{\sqrt{\Omega^2 + \frac{32}{3}g^2}} \right)} \\ \sin \gamma &= \sqrt{\frac{1}{2} \left(1 - \frac{\Omega}{\sqrt{\Omega^2 + \frac{32}{3}g^2}} \right)} \end{aligned} \quad (35)$$

The analysis to this point would be identical if the static bipolarons were in a triplet state. The last case, namely that of an onsite bipolaron, is however only possible for a singlet state. In this case, there are again only 4 polarization clouds, as for a polaron. However, because the charge creating the electric field is doubled, we now replace $g \rightarrow 2g$. As a result, the energy of the on-site bipolaron is:

$$E_{BP,0} = 4 \left[\Omega - \sqrt{\Omega^2 + 16g^2} \right] \quad (36)$$

The effective on-site interaction is then:

$$U_0 = U_H + E_{BP,0} - E_{BP,\infty} = U_H - 4 \left[\sqrt{\Omega^2 + 16g^2} + \Omega - 2\sqrt{\Omega^2 + 4g^2} \right] \quad (37)$$

where U_H is the on-site Hubbard repulsion between the two charges. Clearly, the polarization of neighboring As atoms always acts to screen out the on-site repulsion, and this effect can be very significant. Indeed, in Fig. 11 we plot this renormalization energy, which is several eV for typical parameters of interest to us.

One more comment is in order. In the linear regime, this renormalization energy would be $\approx -16g^2/\Omega \approx -16eV$, which is similar to the values used in Ref. [1]. The smaller values we find here are a direct consequence of the non-linear effects, which are accounted for our this model.

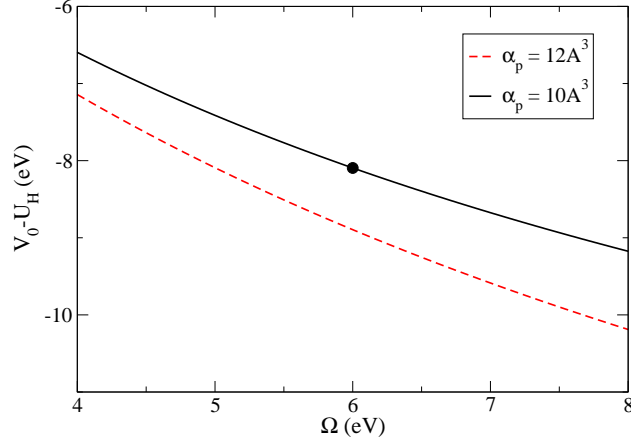


FIG. 11: Renormalization of the on-site interaction $U_0 - U_H$ vs. Ω , for two values of the polarizability. This is always a large attractive contribution, which significantly screens the on-site Hubbard repulsion. The dot shows the typical value we use.

The cloud operators for the on-site bipolaron are similar to the original polaron cloud operators:

$$\tilde{\gamma}_{i,\lambda,\pm,\sigma}^\dagger = \cos \delta s_{i,\sigma}^\dagger - \sin \delta \left[\pm \sin \theta p_{i,\lambda,\sigma}^\dagger + \cos \theta p_{i,3,\sigma}^\dagger \right] \quad (38)$$

where $\lambda = 1$ or 2 depending on the in-plane alignment of the cloud, and \pm reflects its orientation. The only difference is the new mixing angle:

$$\begin{aligned} \cos \delta &= \sqrt{\frac{1}{2} \left(1 + \frac{\Omega}{\sqrt{\Omega^2 + 16g^2}} \right)} \\ \sin \delta &= \sqrt{\frac{1}{2} \left(1 - \frac{\Omega}{\sqrt{\Omega^2 + 16g^2}} \right)} \end{aligned} \quad (39)$$

To summarize, this calculation reveals that for the parameters of interest to us, we can have a stable on-site bipolaron if the Hubbard repulsion is not too large. The nearest-neighbor bipolaron is bound, whereas the 2nd nearest neighbor bipolaron is unstable to dissociation into two free polarons.

B. First order perturbation: effective hopping integrals

We continue the discussion for singlet bipolarons, and analyze how the hopping Hamiltonian mixes together the low energy bipolaron states $s_{i,i+\vec{\delta}}^\dagger |i, i + \vec{\delta}\rangle$. In this notation, $\vec{\delta}$ measures the distance between the two charges, and the state $|i, i + \vec{\delta}\rangle$ describes the As

atoms when there are charges at Fe sites i and $i + \vec{\delta}$. Similar to the states $|i\rangle$ defined for single polarons, the states $|i, i + \vec{\delta}\rangle$ have all As atoms which are not nearest neighbors to either Fe_i or $\text{Fe}_{i+\vec{\delta}}$ in their ground state, while the As atoms in the vicinity of the charged Fe atoms are described by the appropriate $\gamma^\dagger, \tilde{\gamma}^\dagger, \tilde{\tilde{\gamma}}^\dagger$ or $\tilde{\tilde{\gamma}}^\dagger$ operator, as detailed in the previous section. We do not list these expressions explicitly here, as they are rather long and tedious but otherwise straightforward.

From these states, we can define a basis of bipolaron states invariant to translations on the $N \times N$ unit cells lattice:

$$|\vec{k}, \vec{\delta}\rangle = \sum_i \frac{e^{i\vec{k}\cdot(\vec{R}_i + \frac{\vec{\delta}}{2})}}{N} s_{i, i+\vec{\delta}}^\dagger |i, i + \vec{\delta}\rangle. \quad (40)$$

Here \vec{k} is the center-of-mass momentum of the bipolaron pair. It can take the usual equally-spaced values inside the Brillouin zone allowed by the periodic boundary conditions. However, some care needs to be taken in the definition of $\vec{\delta}$, since if we take all its possible values, we double-count the states (for example, $|\vec{k}, \vec{e}_x\rangle = |\vec{k}, -\vec{e}_x\rangle$, etc). This is due to the fact that $\vec{\delta}$ is like a nematic vector, with a size and orientation but without a pointing arrow. Let $\vec{\delta} = \delta_x \vec{e}_x + \delta_y \vec{e}_y$, and for simplicity assume that the lattice size is an odd number, $N = 2n + 1$. Then, double-counting is avoided provided that when $\delta_x = 0$, we allow $\delta_y = 0, 1, \dots, n$ (because of the periodic boundary conditions, the distance between charges cannot be more than half the dimension of the system). If $\delta_x = 1, 2, \dots, n$, then $\delta_y = -n, \dots, n$. Both positive and negative values are needed in this case, because, for example, the $|\vec{k}, \vec{e}_x + \vec{e}_y\rangle$ state is distinct from the $|\vec{k}, \vec{e}_x - \vec{e}_y\rangle$ state, however these are the only two distinct states of the 2nd nearest neighbor bipolarons. In conclusion, for a $N \times N$ lattice with $N = 2n + 1$, there are $(n + 1)(2n + 1) - n$ distinct singlet eigenstates corresponding to a given total momentum \vec{k} (the remaining are triplet states. Similar accounting can be done for lattices with even number of sites).

Because our total Hamiltonian is also invariant to translations, it will not mix states with different momenta. Therefore, we can solve the problem separately in each \vec{k} subspace, and only need to calculate the various $\langle \vec{k}, \vec{\delta}' | \mathcal{H} | \vec{k}, \vec{\delta} \rangle$ matrix elements. There are three sets of such contributions. First, there are ‘‘diagonal’’ contributions, already discussed in the previous section. Specifically, $\langle \vec{k}, \vec{\delta} | \mathcal{H} | \vec{k}, \vec{\delta} \rangle = \langle \vec{k}, \vec{\delta} | \hat{U} + \mathcal{H}_{\text{As}} + \mathcal{H}_{\text{int}} | \vec{k}, \vec{\delta} \rangle = U_{\vec{\delta}}$ where U_0, U_1 and U_2 of Eqs. (29), (33) and (37) correspond to $\vec{\delta}$ indicating, respectively, an on-site, a nearest neighbor or a 2nd nearest neighbor bipolaron state. If $|\vec{\delta}| \geq 2$, then $U_{\vec{\delta}} = 0$, since we

measure the interactions energies with respect to the energy of two unbound static polarons.

The nn hopping Hamiltonian links states with the same momentum but bipolaron distances $\vec{\delta}$ and $\vec{\delta}'$ which are nearest neighbor, *i.e.* $|\vec{\delta} - \vec{\delta}'| = 1$. We therefore also need to calculate these matrix elements $\langle \vec{k}, \vec{\delta} \pm \vec{e}_{x/y} | \mathcal{H} | \vec{k}, \vec{\delta} \rangle = \langle \vec{k}, \vec{\delta} \pm \vec{e}_{x/y} | \hat{T} | \vec{k}, \vec{\delta} \rangle$. Similarly, for finite t' there are matrix elements of \hat{T}' between 2nd nearest neighbor states with $|\vec{\delta} - \vec{\delta}'| = \sqrt{2}$. Taken together, these three sets exhaust all matrix elements which are finite and therefore we can diagonalize the resulting matrix and find the energies and eigenstates corresponding to any desired \vec{k} , within first order perturbation theory.

If $\vec{\delta}$ is large enough, the hopping Hamiltonian \hat{T} will hop one of the electrons away from its clouds, while the second one remains unperturbed. As a result, one expects the matrix element to be proportional to the t_{eff} of the single polaron. Indeed, explicit calculation shows that if the separation $\vec{\delta}$ is at least that of a 3rd nearest neighbor bipolaron, then:

$$\begin{aligned} \langle \vec{k}, \vec{\delta} + \vec{e}_x | \hat{T} | \vec{k}, \vec{\delta} \rangle &= -2t_{\text{eff}} \cos \frac{k_x a}{2} \\ \langle \vec{k}, \vec{\delta} \pm \vec{e}_y | \hat{T} | \vec{k}, \vec{\delta} \rangle &= -2t_{\text{eff}} \cos \frac{k_y a}{2} \end{aligned} \quad (41)$$

The cosine factors appear because of the phases in the definitions of the eigenstates $|\vec{k}, \vec{\delta}\rangle$, which change when the singlet separation $\vec{\delta}$ changes. Given the restrictions on the allowed values of $\vec{\delta}$, one needs to be a bit careful near the boundary of allowed values. For example, based on the definition of Eq. (41), it is straightforward to check that

$$|\vec{k}, \delta_x \vec{e}_x + (n+1)\vec{e}_y\rangle = e^{ik_y a \frac{2n+1}{2}} |\vec{k}, \delta_x \vec{e}_x - n\vec{e}_y\rangle.$$

Given the periodic boundary conditions, the allowed values for momentum, if $N = 2n + 1$, are $k_y a = 2\pi n_y / (2n + 1)$, and the phase factor linking the two states can only be ± 1 . This sign is important because hopping in the y -direction links the state with $\delta_y = n$ to that with $\delta_y = n + 1$, however the later one is not amongst the allowed $\vec{\delta}$ values. The identity above links it to an allowed value, but also introduces a phase shift (the sign) which is transferred to the corresponding matrix element. A similar situation arises for hopping in the x direction when $\delta_x = n$, $\delta_x = 0$ and hopping in the y direction for $\delta_y = -n$. Finally, it is important to note that these phase shifts are different for triplet states (they have opposite sign in most cases, but not all). Other than this (and the non-existence of an triplet onsite bipolaron, as already discussed), essentially everything else is the same for triplet states.

Different effective hopping integrals appear when the electrons are closer together. For nearest-neighbor hopping, there are four such special cases. The first corresponds to hopping from 3rd nearest neighbor to nearest neighbor bipolaron. A straightforward calculation of the overlap of the corresponding polarization clouds leads to an effective hopping:

$$t_3 = t \langle i, i + \vec{e}_x | i, i + 2\vec{e}_x \rangle = t \left[\cos \alpha (\cos^2 \alpha + \sin^2 \alpha \sin^2 \theta) \right]^4 \\ \times \left[\cos \alpha \cos \gamma + \sin \alpha \sin \gamma \left(\frac{\cos \theta}{\sqrt{2}} + \frac{\sin \theta}{2} \right) \right]^4 \quad (42)$$

The matrix elements for such processes are:

$$\langle \vec{k}, 2\vec{e}_x | \hat{T} | \vec{k}, \vec{e}_x \rangle = -2t_3 \cos \frac{k_x a}{2} \\ \langle \vec{k}, 2\vec{e}_y | \hat{T} | \vec{k}, \vec{e}_y \rangle = -2t_3 \cos \frac{k_y a}{2}, \quad (43)$$

in other words like the general matrix elements of Eq. (41), except with the appropriate value of the effective hopping integral.

The second special case involves hopping between 2nd and 4th nn bipolarons. In this case, the overlap between the corresponding polarization clouds leads to:

$$t_4 = t \langle i, i + \vec{e}_x + \vec{e}_y | i, i + \vec{e}_x + 2\vec{e}_y \rangle = t \cos^6 \alpha \left[\cos^2 \alpha + \sin^2 \alpha \cos^2 \theta \right]^4 \\ \times [\cos \alpha \cos \beta + \sin \alpha \sin \beta \cos \theta]^2 \quad (44)$$

and the matrix elements:

$$\langle \vec{k}, 2\vec{e}_x \pm \vec{e}_y | \hat{T} | \vec{k}, \vec{e}_x \pm \vec{e}_y \rangle = -2t_4 \cos \frac{k_x a}{2} \\ \langle \vec{k}, \vec{e}_x \pm 2\vec{e}_y | \hat{T} | \vec{k}, \vec{e}_x \pm \vec{e}_y \rangle = -2t_4 \cos \frac{k_y a}{2}. \quad (45)$$

The third special case involves hopping between 2nd and 1st nearest neighbor bipolarons. In this case, the overlap between the polarization clouds corresponding to these two cases leads to a renormalized hopping:

$$t_2 = t \langle i, i + \vec{e}_x | i, i + \vec{e}_x + \vec{e}_y \rangle = t \cos^6 \alpha \left[\cos^2 \alpha + \sin^2 \alpha \cos^2 \theta \right]^2 \left[\cos \beta \cos \gamma + \frac{\sin \beta \sin \gamma}{\sqrt{2}} \right]^2 \\ \times \left[\cos \alpha \cos \gamma + \sin \alpha \sin \gamma \left(\frac{\cos \theta}{\sqrt{2}} + \frac{\sin \theta}{2} \right) \right]^2 \quad (46)$$

and the matrix elements:

$$\langle \vec{k}, \vec{e}_x \pm \vec{e}_y | \hat{T} | \vec{k}, \vec{e}_y \rangle = -2t_2 \cos \frac{k_x a}{2} \\ \langle \vec{k}, \vec{e}_x \pm \vec{e}_y | \hat{T} | \vec{k}, \vec{e}_x \rangle = -2t_2 \cos \frac{k_y a}{2}. \quad (47)$$

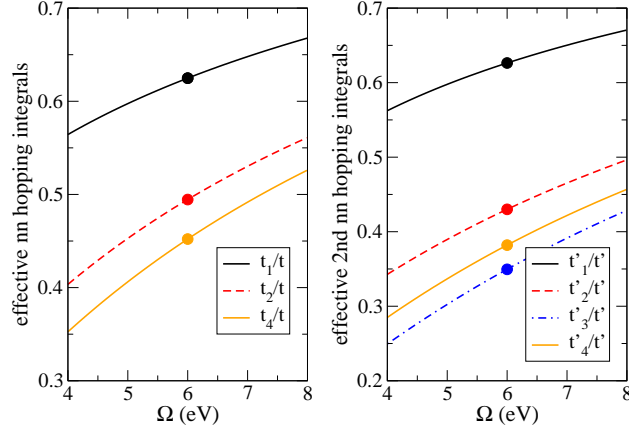


FIG. 12: Effective hoppings for closely-spaced bipolarons. For these parameters, the t_2 and t_3 curves are essentially superimposed, therefore we only show t_2/t .

Finally, for the hopping between on-site and nearest neighbor bipolaron, the effective hopping is found to be:

$$t_1 = t \langle i, i | i, i + \vec{e}_x \rangle = t \cos^4 \alpha \cos^4(\alpha - \delta) \left[\cos \delta \cos \gamma + \sin \delta \sin \gamma \left(\frac{\cos \theta}{\sqrt{2}} + \frac{\sin \theta}{2} \right) \right]^4 \quad (48)$$

and the matrix elements are:

$$\begin{aligned} \langle \vec{k}, \vec{e}_x | \hat{T} | \vec{k}, 0 \rangle &= -2\sqrt{2}t_1 \cos \frac{k_x a}{2} \\ \langle \vec{k}, \vec{e}_y | \hat{T} | \vec{k}, 0 \rangle &= -2\sqrt{2}t_1 \cos \frac{k_y a}{2}. \end{aligned} \quad (49)$$

The extra factor of $\sqrt{2}$ is because of the on-site singlet normalization, see Eq. (26). Of course, for triplet states $t_1 = 0$, since there is no on-site triplet.

In Fig. 12(a) we plot the values of $t_1/t, t_2/t, t_3/t$ and t_4/t vs. Ω for $\alpha_P = 10\text{\AA}^3$. These should be compared with t_{eff}/t shown in Fig. 6. The overall changes are relatively small.

The situation for second nearest neighbor hopping is similar. If $\vec{\delta}$ is large enough, then the cloud overlap is the same as for individual polarons and the renormalized hopping is t'_{eff} , giving the matrix elements:

$$\langle \vec{k}, \vec{\delta} + \vec{e}_x \pm \vec{e}_y | \hat{T}' | \vec{k}, \vec{\delta} \rangle = -2t'_{\text{eff}} \cos \frac{(k_x \pm k_y)a}{2} \quad (50)$$

Again, special care must be used for values of $\vec{\delta}$ near the edges of its area of allowed values, so that the periodic boundary conditions are properly accounted for. This is done in a manner totally analogous to that explained for nearest neighbor hopping.

There are again four special cases of different renormalization of t' . One involves the hopping between the two possible nearest-neighbor bipolaron states, which has the matrix element:

$$\langle \vec{k}, \vec{e}_x | \hat{T}' | \vec{k}, \vec{e}_y \rangle = -2t'_2 \left[\cos \frac{(k_x + k_y)a}{2} + \cos \frac{(k_x - k_y)a}{2} \right] \quad (51)$$

where

$$t'_2 = t' \langle i, i+x | i, i+y \rangle = t' [\cos \alpha]^8 \left[\cos \alpha \cos \gamma + \sin \alpha \sin \gamma \left(\frac{\cos \theta}{\sqrt{2}} + \frac{\sin \theta}{2} \right) \right]^4 \left[\cos^2 \gamma + \frac{1}{2} \sin^2 \gamma \right]^2 \quad (52)$$

The second involves the hopping between 2^{nd} and 3^{rd} nn bipolarons, as well as hopping away from a 2^{nd} nn bipolaron, with the matrix elements:

$$\begin{aligned} \langle \vec{k}, 2\vec{e}_x \pm 2\vec{e}_y | \hat{T}' | \vec{k}, \vec{e}_x \pm \vec{e}_y \rangle &= -2t'_3 \cos \frac{(k_x \pm k_y)a}{2} \\ \langle \vec{k}, 2\vec{e}_x | \hat{T}' | \vec{k}, \vec{e}_x \pm \vec{e}_y \rangle &= -2t'_3 \cos \frac{(k_x \mp k_y)a}{2} \\ \langle \vec{k}, 2\vec{e}_y | \hat{T}' | \vec{k}, \vec{e}_x \pm \vec{e}_y \rangle &= -2t'_3 \cos \frac{(k_x \mp k_y)a}{2} \end{aligned} \quad (53)$$

$$(54)$$

where $t'_3 = t' \langle i, i+x+y | i, i+2x+2y \rangle = t' \langle i+x+y | i+2x \rangle$ is found to be:

$$t'_3 = t' [\cos \alpha]^{10} [\cos \alpha \cos \beta + \sin \alpha \sin \beta \cos \theta]^2 [\cos^2 \alpha + \sin^2 \alpha \cos(2\theta)]^2 \quad (55)$$

The third case involves hopping between 1^{st} and 4^{th} nn bipolarons, with matrix elements:

$$\begin{aligned} \langle \vec{k}, 2\vec{e}_x \pm \vec{e}_y | \hat{T}' | \vec{k}, \vec{e}_x \rangle &= -2t'_4 \cos \frac{(k_x \pm k_y)a}{2} \\ \langle \vec{k}, \vec{e}_x \pm 2\vec{e}_y | \hat{T}' | \vec{k}, \vec{e}_y \rangle &= -2t'_4 \cos \frac{(k_x \pm k_y)a}{2} \end{aligned} \quad (56)$$

$$(57)$$

where $t'_4 = t' \langle i+x | i+2x+y \rangle$ equals:

$$t'_4 = t' [\cos \alpha]^8 [\cos^2 \alpha + \sin^2 \alpha \cos(2\theta)]^2 \left[\cos \alpha \cos \gamma + \sin \alpha \sin \gamma \left(\frac{\cos \theta}{\sqrt{2}} + \frac{\sin \theta}{2} \right) \right]^4. \quad (58)$$

Finally, the hopping between an on-site and a 2nd nearest neighbor bipolaron (again, possible only for singlet states) leads to:

$$\langle \vec{k}, \vec{e}_x \pm \vec{e}_y | \hat{T}' | \vec{k}, 0 \rangle = -2\sqrt{2}t'_1 \cos \frac{(k_x \pm k_y)a}{2} \quad (59)$$

where

$$t'_1 = t' \langle i, i | i, i + x + y \rangle = t' [\cos \alpha \cos(\alpha - \delta)]^6 [\cos(\beta - \delta)]^2. \quad (60)$$

The renormalized values t'_1, t'_2, t'_3 and t'_4 are shown, in units of t' , in Fig. 12(b).

The ensemble of all these matrix elements define the matrix that needs to be diagonalized in order to find eigenstates and eigenvalues for a given total momentum \vec{k} . The results are shown in the main paper.

IV. ESTIMATES FOR THE ACCURACY OF VARIOUS APPROXIMATIONS

In the previous sections we argued that first order perturbation theory is reasonably accurate for our Hamiltonian, given the values of the various parameters relevant for the Fe-based superconductors. However, the Hamiltonian itself already embodies two approximations, namely (i) that only As atoms nn to a doping charge become polarized, and (ii) that dipole-dipole interactions between the various polarized As atoms are ignored.

We provide here rough estimates for the accuracy of these approximations. We begin by discussing the single polaron.

Assume that interactions with the 8 As atoms which are 2^{nd} nn to a charge are also included. This supplementary interaction would be described by a Hamiltonian similar to \mathcal{H}_{int} of Eq. (3), except it would have a new energy scale g' and new angles describing the orientations of these Fe-As bonds.

From the definition of the interaction energy, Eq. (7), we have:

$$\frac{g'}{g} = \frac{R^2}{R'^2}$$

where $R' = \sqrt{11}a/2$ is the distance from an Fe to a 2^{nd} nn As atom. This comes about because the only difference is in the electric fields created at the two sites, and these are inversely proportional to the square of the distances.

It then follows immediately that the contribution to the static polaron energy of these 8 clouds would be:

$$E_{\text{corr}} = 8 \left(\Omega - \sqrt{\Omega^2 + 4g'^2} \right), \quad (61)$$

which for our typical parameters is $E_{\text{corr}} = -1.2$ eV. Of course, considering the polarization of even more distant As atoms would lower this energy even more.

However, this decrease is more than compensated for by consideration of dipole-dipole interactions. To estimate these energies, let us consider only the 6 pair interactions between the 4 largest dipole moments on the nn As sites. Consider a pair of two such dipoles, with moments \vec{p}_1 and \vec{p}_2 . Their magnitude is given by Eq. (13) and their orientations are straightforward to determine, as is the distance \vec{d} between them. Using these values, we find for any such pair that:

$$E_{d-d} = \frac{1}{d^3} \left(\vec{p}_1 \cdot \vec{p}_2 - 3 \frac{(\vec{p}_1 \cdot \vec{d})(\vec{p}_2 \cdot \vec{d})}{d^2} \right) = \frac{10\alpha_p\Omega}{3\sqrt{2}a^3} \frac{g^2}{\Omega^2 + 4g^2} \quad (62)$$

where the numerical factor in front is due to geometrical considerations. For our typical parameters, $E_{d-d} = 0.66\text{eV}$ and therefore the total for the 6 pair interactions is $\approx 4\text{ eV}$. Inclusion of contributions from interactions with the dipoles on the 2^{nd} nn As atoms will decrease this, because nn and 2^{nd} nn dipoles closest to each other are now roughly parallel, not anti-parallel, to each other.

Taken together and without further corrections, these two energies would renormalize $E_{B,PS}$ to about half the value predicted in their absence. If we keep adding further rows of neighbors into the calculation, the polaron energy saturates (slowly) to around -1.6eV (of course, if the fields decrease as $1/R^2$, the energy slowly become more negative and will eventually go to $-\infty$. However one has to take into account that there are other screening mechanism that further screen the interaction). Having extended clouds would also lower the effective hoppings somewhat more, although we expect this to be a much smaller effect: clouds which are far from the electronic charge are changed much if the charge moves by one site. As a result, their contribution to the total overlap should be very close to 1.

Although the renormalization of the static part of the polaron energy is quite substantial, these corrections do not have nearly as large an effect on the bipolaron interaction energies U_0, U_1 and U_2 . The reason is that these are differences between the true bipolaron energy and the energy of two free polarons, and therefore many contributions from both the extended clouds and the dipole-dipole interactions cancel each other out.

For example, consider the effects of these corrections on U_1 , which is the most interesting energy. For two polarons at an infinite distance from each other, the dipole-dipole correction is $12 E_{d-d}$ and there are a total of $16 \cdot 2^{nd}$ nn extra clouds. For a nn bipolaron, the dipole-dipole energy is roughly $11 E_{d-d}$, because the two As tetrahedra share one side (of course, the two central As atoms have somewhat different dipole moments pointing in somewhat

different directions, and also there are smaller contributions from interactions between the non-central As atoms belonging to different Fe, but 11 E_{d-d} should be a reasonable guess). This configuration would only have 12 2^{nd} nn extra clouds. Subtracting these corrections leads to an overall correction of U_1 roughly equal to $-\frac{1}{2}E_{corr} - E_{d-d} \approx 0$. In reality, the energy is lowered because the close location of the two charges implies larger electric fields at all sites for the nn bipolaron, therefore larger clouds. We find that as we increase the number of As neighbors included in the cloud, U_1 is lowered from ≈ -1 eV (the value we find when the approximations are made) to -2.87 eV if we include 2nd nn and dipole-dipole interactions, to -4 eV if more and more neighbors are added. Again, one expects that the electric fields will be screened over some finite distance which will decide the precise value. The point, though, is that relaxing the approximations increases this attraction energy, in other words the physics we discuss here becomes more relevant, not less.

V. LINK BETWEEN BCS-LIKE THEORY AND EXPERIMENTAL DATA

There have been many works in the recent experimental literature pointing to correlations between the critical temperature T_c and shorter Fe-As distances and smaller Fe-As-Fe angles, see for example Ref. 3. Such correlations would come as a natural consequence in our theory, where the “glue” leading to pair formation is the polarization of nearby As ions, and thus it is very sensitive to the precise location of the As with respect to Fe.

As discussed towards the end of our main paper, we currently envision two possible scenarios explaining the high- T_c in the materials, namely a BCS-like and a BEC-like scenario. The BEC-like scenario assumes that the nearest-neighbor attraction U_1 is larger than the nearest-neighbor bare Coulomb repulsion (not included in our simulations) and that pre-formed bosonic pairs appear well above T_c . As discussed, there is experimental evidence consistent with this scenario. The BCS-like scenario assumes that the nn Coulomb repulsion is large enough to overcome U_1 , and therefore there are no pre-formed pairs in the system. However, like in regular superconductors, the existence of an attraction mechanism (given by U_1), when combined with the existence of a Fermi sea and proper inclusion of retardation effects, should suffice to lead to Cooper-pair formation at T_c .

Currently, our calculations are not detailed enough to allow us to distinguish which scenario is the more likely one. In this section we first *speculate* on the possible fit of the

experimental data to the BCS-like scenario, and then comment on the relevance of the same data for the BEC scenario.

The well-known BCS formula links T_c to the typical scale of the attractive potential V in an exponential dependence, $T_c \sim \exp\left(-\frac{1}{|V|\rho}\right)$, where ρ is the density of states at the Fermi energy. On a logarithmic scale, this implies $\ln T_c = \text{const.} - \frac{1}{|V|\rho}$, if we assume that the prefactor is roughly constant. For simplicity, let us also assume that $V \propto U_1 \propto \alpha_p \vec{E}_1 \cdot \vec{E}_2 \propto \alpha_p \frac{\cos \gamma}{R^4}$, where R is the Fe-As distance and γ is the nn Fe-As-Fe angle. As explained in the main paper, this expression gives the linear approximation for the nn U_1 attraction [1], and we use it here for simplicity – since we will ignore changes in the density of states for the various materials, taking into consideration the small non-linear effects is superfluous.

In Fig. 13 we show a plot of T_c vs. $\frac{R^4}{\alpha_p \cos \gamma}$ for a multitude of materials, which have polarizabilities, R and γ values varying over fairly large ranges [3, 4, 5, 6, 7, 8, 9, 10, 11, 12, 13, 14, 15, 16]. While there is some spread to the data, it is not inconsistent with a linear dependence like that predicted by a BCS formula. Of course, a lot more theoretical work needs to be done before one could justify this plot as more than just an accident.

This sensitivity of T_c to α_p , R and γ is not inconsistent with a BEC-like scenario, either. Assuming that U_1 is large enough that pre-formed pairs exist up to very high temperatures, then T_c would be related to the on-set of coherence between these bosons. Generally speak-

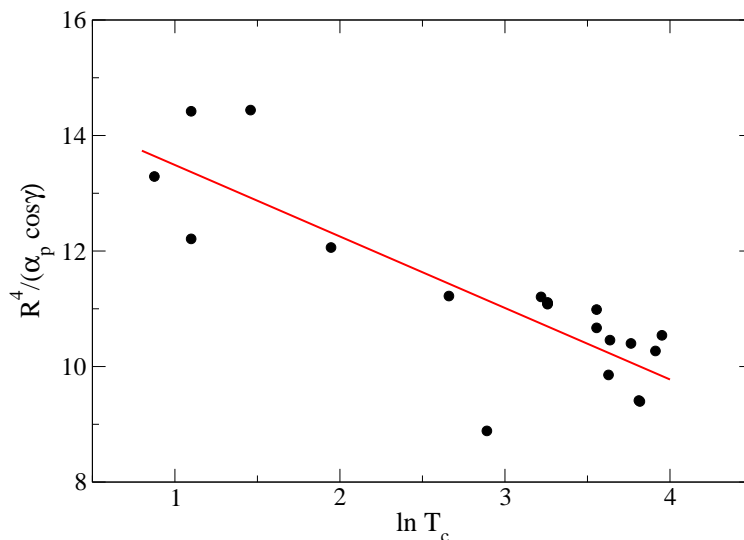


FIG. 13: Linear fit of $\ln T_c$ vs. $\frac{R^4}{\alpha_p \cos \gamma}$. The data points are taken from Refs. 3, 4, 5, 6, 7, 8, 9, 10, 11, 12, 13, 14, 15, 16.

ing, this is achieved when the de Broglie wavelength becomes comparable to the average spacing between bosons. Whatever the specific relationship is, it will involve the effective mass of these pre-formed pairs. This effective mass depends in a non-trivial fashion on α_p , R and γ , as discussed in the main paper. This dependence is not only through U_1 , but to a large degree also through the cloud overlaps determining the various t_{eff} values. Since all these quantities are very sensitive to α_p , R and γ , this scenario would also be compatible with a T_c which depends on these quantities. Trying to fit it would, at this point, be even more speculative than the fit shown in Fig. 13.

In any event, the underlying idea is that if the As ions played a small, secondary-type role in determining the behavior of these materials, this dependence would be very puzzling. In our model, the As anions are the main enablers of the pairing mechanics, therefore this sensitivity of T_c to specific details of the lattice structure follows quite naturally.

-
- [1] Sawatzky, G. A. , Elfimov I.S., van den Brink J., Zaanen J. Heavy anion solvation of polarity fluctuations in Pnictides. Preprint at <http://arxiv.org/abs/0808.1390> (2008).
 - [2] Lu, D. H. *et al.* Electronic structure of the iron-based superconductor LaOFeP. *Nature* **455**, 81-84 (2008).
 - [3] Zhao, J. *et al.* Structural and magnetic phase diagram of CeFeAsO_{1-x}F_x and its relationship to high-temperature superconductivity. Preprint at <http://arxiv.org/abs/0806.2528> (2008).
 - [4] Qiu, Y. *et al.* Neutron scattering study of the oxypnictide superconductor La(O,F)FeAs. Preprint at <http://arxiv.org/abs/0805.1062> (2008).
 - [5] Huang, Q. *et al.* Doping evolution of antiferromagnetic order and structural distortion in LaFeAsO_{1-x}F_x. Preprint at <http://arxiv.org/abs/0809.4816> (2008).
 - [6] Sefat, A. S. *et al.* Superconductivity in Co-doped LaFeAsO. Preprint at <http://arxiv.org/abs/0807.0823> (2008).
 - [7] Bos, J-W. G. *et al.* High pressure synthesis of late rare earth RFeAs(O,F) superconductors; R = Tb and Dy. *Chem. Commun* **31**, 3634-3635 (2008).
 - [8] de la Cruz, C. *et al.* Magnetic order close to superconductivity in the iron-based layered LaO_{1-x}F_xFeAs systems. *Nature* **453**, 899 (2008).
 - [9] Qiu, Y. *et al.* Structure and Magnetic Order in the NdFeAs(O,F) Superconductor System .

- Preprint at <http://arxiv.org/abs/0806.2195> (2008).
- [10] Tapp, J.H. *et al.* LiFeAs: An Intrinsic FeAs-based Superconductor with $T_c = 18\text{K}$. Preprint at <http://arxiv.org/abs/0807.2274> (2008).
- [11] Tegel, M. *et al.* A ^{57}Fe Moessbauer Spectroscopy Study of the 7 K Superconductor LaFePO. Preprint at <http://arxiv.org/abs/0805.1208> (2008).
- [12] Watanabe, T. *et al.* Nickel-Based Oxyphosphide Superconductor with a Layered Crystal Structure, LaNiOP, *Inorg. Chem.* **46**, 7719-7721 (2007).
- [13] Tegel, M. *et al.* Synthesis, crystal structure and superconductivity of LaNiPO. *Solid State Sci.* **10**, 193-197 (2007).
- [14] Mine, T. *et al.* Nickel-based phosphide superconductor with infinite-layer structure, BaNi 2 P 2 . *Solid State Commun.* **147**, 111-113 (2008).
- [15] Zhao, J. *et al.* Lattice and magnetic structures of PrFeAsO, PrFeAsO $_{0.85}$ F $_{0.15}$, and PrFeAsO $_{0.85}$. *Phys. Rev. B* **78**, 132504 (2008).
- [16] Watanabe, T. *et al.* Nickel-based layered superconductor, LaNiOAs. *J. Solid State Chem.* **181**, 2117-2120 (2008).